5 Climate of the Mediterranean: Synoptic Patterns, Temperature, Precipitation, Winds, and Their Extremes

Uwe Ulbrich[a], Piero Lionello[b], Danijel Belušić[c], Jucundus Jacobeit[d], Peter Knippertz[e], Franz G. Kuglitsch[f], Gregor C. Leckebusch[g], Jürg Luterbacher[h], Maurizio Maugeri[i], Panagiotis Maheras[j], Katrin M. Nissen[a], Valentina Pavan[k], Joaquim G. Pinto[l], Hadas Saaroni[m], Stefanie Seubert[d], Andrea Toreti[h], Elena Xoplaki[f], Baruch Ziv[n]

[a]Institut für Meteorologie, Freie Universität Berlin, Germany, [b]University of Salento, Lecce, Italy and CMCC, Italy, [c]School of Mathematical Sciences, Monash University, Victoria, Australia, [d]Institute of Geography, University of Augsburg, Augsburg, Germany, [e]Institute for Atmospheric Physics, Johannes Gutenberg University, Mainz, Germany, [f]Institute of Geography and Oeschger Centre for Climate Change Research, University of Bern, Bern, Switzerland, [g]School of Geography, Earth and Environmental Sciences, University of Birmingham, Birmingham, UK, [h]Department of Geography, Justus-Liebig University of Giessen, Giessen, Germany, [i]Dipartimento di Fisica, Università degli studi di Milano, Milan, Italy, [j]Department of Meteorology and Climatology, Aristotle University of Thessaloniki, Thessaloniki, Greece, [k]ARPA-SIMC, Bologna, Italy, [l]Institute for Geophysics and Meteorology, University of Cologne, Cologne, Germany, [m]Department of Geography and the Human Environment, Tel Aviv University, Tel Aviv, Israel, [n]Department of Natural Sciences, The Open University of Israel, Raanana, Israel

5.1 Introduction

In this chapter, regional climate conditions are described in terms of the properties and behavior of the atmospheric circulation over and around the Mediterranean region (MR). The aims are to study the relationships between the atmospheric circulation and the surface environment and to identify key dynamical interactions that are involved. In this sense, the content of this chapter belongs to the general topic of synoptic climatology (see Huth et al., 2009 for a short discussion). Specifically

The Climate of the Mediterranean Region. DOI: 10.1016/B978-0-12-416042-2.00005-7

this chapter describes the teleconnection patterns influencing the MR (Section 5.2), the characteristics of the cyclones in the MR and their links to large-scale patterns (Section 5.3), and the synoptic circulation conditions leading to temperature and precipitation extremes (Sections 5.4 and 5.5, respectively). Finally, local winds, wind extremes, and some specific effects they induce (e.g., dust storms, storm surges, and waves) are discussed.

5.2 Teleconnection Patterns Influencing the MR

Variations in weather and climate are organized, in part, into continental scale patterns describing the level of coherent time behavior for a given variable (often the sea-level pressure (SLP) or the 500 hPa geopotential height) as function of space. These patterns, called "teleconnection patterns," are usually described by maps in which areas with high correlation and anticorrelation are shown. Teleconnections are commonly identified from neighboring maxima of anticorrelation (Wallace and Gutzler, 1981) or from principal-component analysis producing such patterns (Barnston and Livezey, 1987). Because of their empirical nature, no distinct threshold can be given for remote distances in this context, but usually they extend at least to several thousands of kilometers. Different temporal scales and time lags may also be involved in such teleconnections. The existence, locations, and characteristics of the patterns can be related to various complex dynamical and thermodynamical influences, which are still subject to ongoing research. It should also be noted that the exact spatial and temporal characteristics of the named pattern (including those mentioned below) are not unique but often differ slightly between studies because of the different methods and data sets used for their identification.

In this section, we will give a short overview of important teleconnections influencing the MR, namely, the North Atlantic Oscillation (NAO), the East Atlantic pattern (EA), the East Atlantic/West Russian pattern (EA/WR or Eurasian Type 1 (EU1); Barnston and Livezey, 1987), and the Scandinavian pattern (SCAND or Eurasian Type 2 [EU2]). The spatial signature of three of the mentioned large-scale patterns (NAO, EA, and SCAND) affecting the Euro-Atlantic region during winter (DJF) is displayed in Figure 5.1.

The NAO, with centers of action near Iceland and the Azores, has long been identified as an influencing factor on Mediterranean climate variability, especially during winter. In the positive phase, the pressure minimum associated with the Icelandic low is deepened, while the pressure maximum associated with the Azores high is enhanced. This phase favors warmer conditions over the northern part and cooler conditions over the southern part of the MR, with an inverse pattern for the negative phase of the NAO (Xoplaki, 2002; Trigo et al., 2002b, 2006). Positive relationships are prevalent over the northwestern Mediterranean coast and central and eastern Europe, with maximum values north of 45°N (Xoplaki, 2002). Toreti et al. (2010a) have reported a significant positive correlation between NAO and north Italian winter temperature. The winter NAO is significantly negative correlated with the air temperature over a huge area in the southeastern part of the Euro-Mediterranean

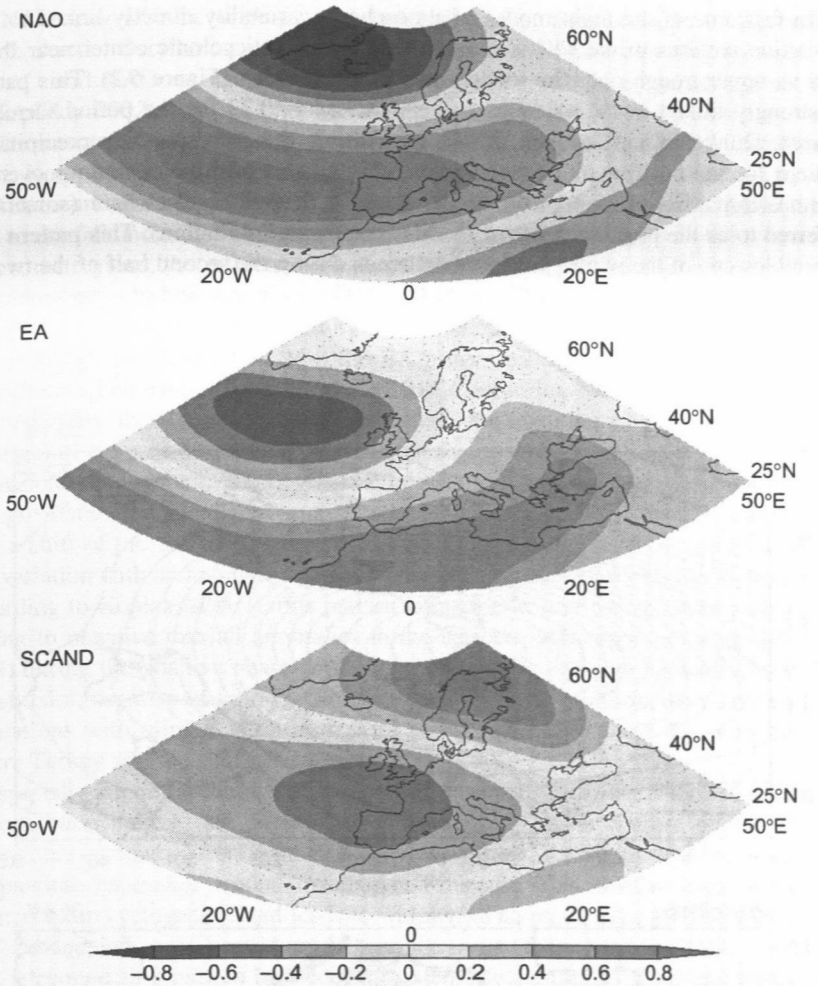

Figure 5.1 Three teleconnection patterns relevant for Mediterranean winter (DJF, 1960–2000) climate variability: NAO, EA, and SCAND based on definitions by Barnston and Livezey (1987).

region, including mid-Algeria, Libya and Egypt, Greece, Turkey (Türkeş and Erlat, 2009), Cyprus, and the entire Near East countries. The areas from southern Iberia, southern Italy, the southern Balkans toward the Black Sea return non-significant correlations with respect to wintertime air temperature.

Still more important is the impact on precipitation variability due to corresponding changes in storm-track activity: the positive winter NAO is related to below-average precipitation rates over large parts of the western and northern MR, with opposite deviations for the negative winter NAO (Ulbrich et al., 1999; Trigo et al., 2004, 2006; Türkes and Erlat, 2003).

In fact, one of the main modes of atmospheric variability directly linked to precipitation patterns in the MR is characterized by an anticyclonic center near Iberia and an upper trough over the southeastern Mediterranean (Figure 5.2). This pattern is strongly linked to the extended winter NAO ($r = 0.72$ for the period October–March; Dünkeloh and Jacobeit, 2003). In addition, the corresponding precipitation pattern for the positive mode (see Figure 5.2) includes positive deviations over the southeastern MR—thus opposite to the negative deviations elsewhere (sometimes referred to as the positive phase of the Mediterranean Oscillation). This pattern also resembles one of the winter precipitation trends during the second half of the twentieth century (Jacobeit et al., 2007) when the NAO was in a period of strong increase.

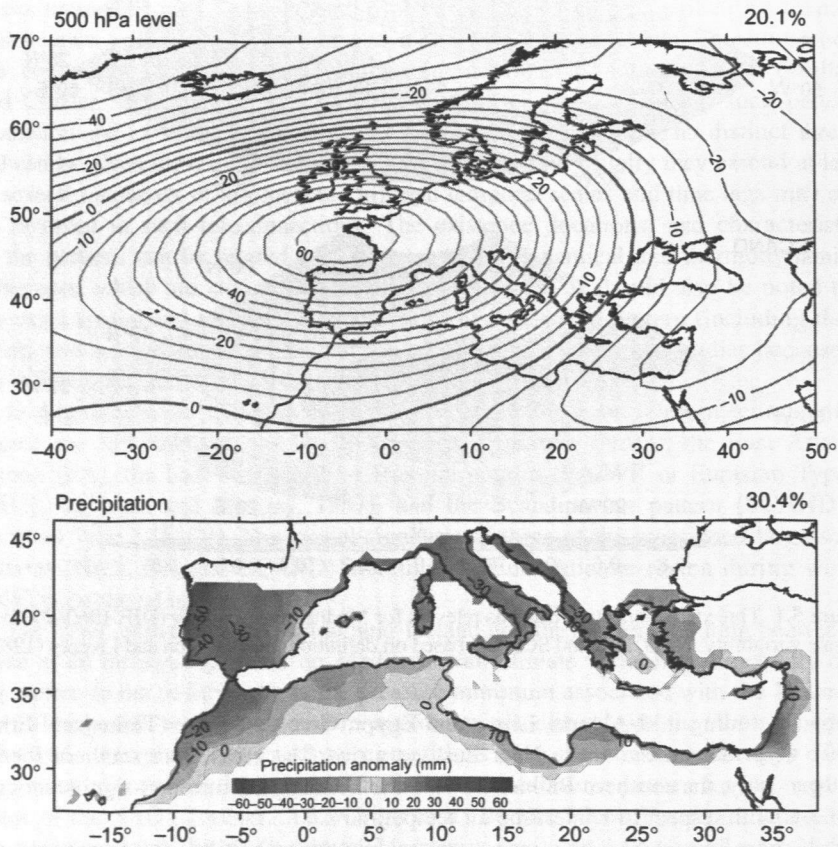

Figure 5.2 First canonical correlation patterns for winter (October–March 1948–1998) related to 500 hPa geopotential heights and Mediterranean precipitation (percentages refer to corresponding explained variances). Correlation coefficient with NAO index (based on CRU data) is 0.72. *Source*: Modified from Dünkeloh and Jacobeit (2003).

The NAO may also be seen as an Atlantic–European manifestation of the hemispheric Arctic Oscillation (AO), corresponding to the fact that the impacts of both AO and NAO on Mediterranean winter climate are quite similar (as shown by Xoplaki, 2002). During the transitional seasons, the NAO influence on the Mediterranean becomes weaker (Dünkeloh and Jacobeit, 2003; Türkes and Erlat, 2003). Knippertz et al. (2003) and Martín et al. (2004) note temporal changes in the NAO structure during this season, resulting in corresponding changes of NAO relations to rainfall anomalies along the southwestern part of the MR.

In some regions, the influence of other teleconnection patterns exceeds that of the NAO. A prominent example is the winter (DJF) temperature variability in the western MR, to a large extent explained by the EA pattern (Sáenz et al., 2001; see Figure 5.1). A significant correlation with the EA pattern has also been identified for the entire Italian Peninsula (Toreti et al., 2010a). Concerning Mediterranean precipitation variability, the EA influence is less distinct, but there are some coupled circulation–rainfall patterns during winter that are being moderately correlated with the EA (Dünkeloh and Jacobeit, 2003). An example is the EA/WR pattern (www.cpc.ncep.noaa.gov/data/teledoc/eawruss_map.shtml), which can be seen as a mode arising from a shift of the EA toward the British Isles, combining this local center of pressure variation with an anomaly center of opposite signature north of the Caspian Sea. According to Xoplaki (2002), this pattern influences winter precipitation variability, leading to negative rainfall anomalies in the northern MR (approximately north of 40°N) during the positive phase of the pattern (positive pressure anomalies near the British Isles, negative ones in the Caspian Sea region). In addition, there are positive correlations with rainfall in an area from northeastern Africa and the Near East to eastern Turkey and the Black Sea region.

Especially important for Mediterranean winter rainfall variability is the Scandinavian teleconnection pattern (see Figure 5.1) characterized—in its positive phase—by an anticyclonic anomaly over Fennoscandia and western Russia as well as by negative pressure anomalies around the Iberian Peninsula. This positive mode enhances Mediterranean cyclogenesis and leads to widespread above-average precipitation in the MR, with maxima in the central-northern region around Italy (Xoplaki, 2002).

A teleconnection pattern between the eastern Mediterranean (EM) and northeastern Atlantic, referred to as the EM pattern, has been identified at the levels 500 and 300 hPa (Hatzaki et al., 2007, 2009). It appears in winter and autumn and has no relationship with the NAO and the Mediterranean Oscillation. The positive phase of this pattern is attributed to the prevalence of high-pressure systems over central Europe, thus causing positive temperature anomalies over northwestern Europe and negative anomalies over northern Africa. It is also associated with an enhanced frequency of northerly flow over Greece, contributing to an increase in precipitation over the EM. Its negative phase is characterized by an increased frequency of anticyclonic flow at 500 hPa over Greece and a consistent tropospheric warming over the same area.

Besides these influences from extratropical latitudes, links of Mediterranean climate variability to tropical circulation anomalies have been identified. The most important one is the relation to the El Niño Southern Oscillation (ENSO), whose

signals from the tropical Pacific area can be propagated downstream as a Rossby-wave train (Alpert et al., 2006), thus affecting regions like the MR, far away from the Pacific origin of the dynamical signal. ENSO influences on the Mediterranean are linked to different stages of the ENSO cycle, depend on the season, occur within the same season or with a time lag amounting to several months to seasons, and differ in the particular mechanisms of large-scale signal transport. Correlations between ENSO and western Mediterranean rainfall have been found for spring and autumn, but with opposite signs: spring rainfall following ENSO warm events is decreased (Rodó et al., 1997; van Oldenborgh et al., 2000; Mariotti et al., 2002), whereas autumn rainfall preceding the mature warm phase of ENSO is increased (Mariotti et al., 2005). There is also evidence for decadal changes of such links during the twentieth century. The correlation between ENSO and North African rainfall apparently vanished during the period 1931–1960 (Knippertz et al., 2003). These variations have been assigned to connections between ENSO and NAO. According to Raible et al. (2004), the variations can be assigned to two modes in the North Atlantic region, one with strong NAO variability and no discernible ENSO influence, and another with a notable influence, associated with strong coupling of ENSO and the Atlantic through the PNA (Pacific/North American) pattern. This link was investigated by Pinto et al. (2011), who suggested that midlatitude cyclones play a major role in the variable connection of PNA and NAO. Links between the Pacific and the EM pattern have also been suggested. The positive phase of this pattern forms when a forcing (tropical heating) appears in the tropical Pacific, along with an anomalous southerly flow over the region of the north Pacific (Hatzaki et al., 2007, 2009). Finally, a statistical relationship between El Niño and European winter temperature has been reported by Brönnimann et al. (2007). Teleconnection mechanisms are supposed to be different for warm and cold ENSO events: anomalous warming in the eastern tropical Pacific is linked with a weak Atlantic Hadley cell (Rodó, 2001) and a (positive) PNA-like circulation pattern between the Pacific and Atlantic Oceans (Mariotti et al., 2005), whereas during La Niña events, tropical Atlantic sea-surface temperature (SST) anomalies may force northeastward-propagating Rossby waves (Mariotti et al., 2005).

Concerning Mediterranean winter precipitation, Pozo-Vásquez et al. (2005) identified a distinct La Niña signal with widespread negative anomalies in southern Europe (most pronounced in southwest Iberia) due to more zonal cyclone tracks in higher midlatitudes and fewer cyclones in the MR. However, the inverse signal for El Niño events—increased winter rainfall—has been detected only for Israel after the mid-1970s (Price et al., 1998), induced by southward shifts of the upper tropospheric jetstream over the EM (Alpert et al., 2006). Finally, even the summer season is affected by ENSO impacts; according to Seubert (2010), an intraannual teleconnection sequence that corresponds to the developing phase of ENSO warm (cold) events has its most distinct influence on Mediterranean rainfall variability from late summer to early autumn, leading to positive (negative) precipitation anomalies as already mentioned above for the conventional autumn season (Mariotti et al., 2005). This influence is linked, with near-surface-pressure anomalies being opposite between the western and the EM (see El Niño and La Niña composites in Figure 5.3 for the period July–October). Thus, the MO being linked to the NAO during winter (referred

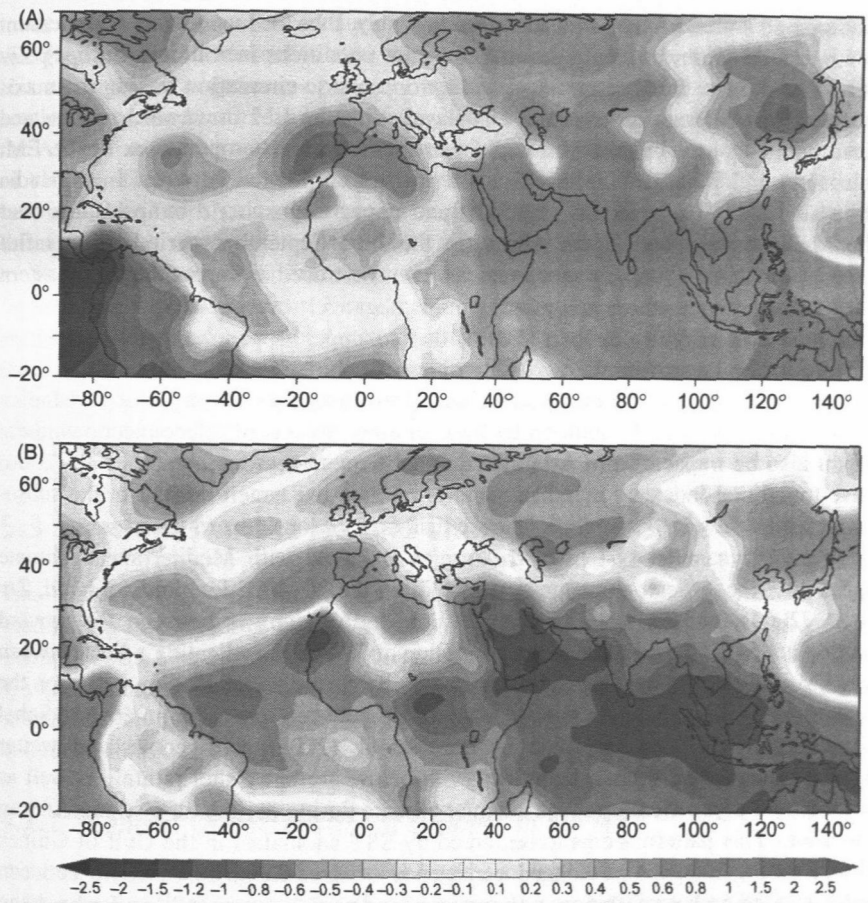

Figure 5.3 Composites of 1000 hPa geopotential height anomalies for El Niño conditions (A, NINO3.4-Index more than 1 standard deviation above the mean value) and for La Niña conditions (B, NINO3.4-Index more than 1 standard deviation below the mean value) during the period July–October 1951–2000.
Source: Modified from Seubert (2010).

to earlier in this chapter) can be attributed (with respect to near-surface pressure) to ENSO variability at least from late summer to early autumn (Seubert, 2010). In addition, Figure 5.3 indicates that there is also a large-scale connection to the Indian summer monsoon (see below).

South Asian monsoon teleconnections have been discussed since the 1990s, and Rodwell and Hoskins (1996) have pointed out an important linkage between the distinct summertime strengthening of descent over the EM and the onset of the South Asian monsoon ("monsoon-desert mechanism") due to a Rossby-wave pattern induced to the west of the diabatic heating in the Asian monsoon region.

Latitudinal shifts of this monsoon heating may thus influence the EM descent (with remote southward shifts leading to wetter conditions in southern Europe). Ziv et al. (2004) have furthermore identified a tropospheric circulation linking the maximum of upward motion over the Himalayas with the EM downward motion and have pointed out a linkage between Asian monsoon and temperatures in the EM. Also, Liu and Yanai (2001) have found a positive correlation between the All-India Rainfall Index (Parthasarathy, 1995a,b) and upper tropospheric temperatures over the Mediterranean and North Africa (in the June–September period). The influence of the Indian summer monsoon can even be traced as far as the northeastern Mediterranean area whose summer rainfall is negatively correlated with Indian summer monsoon rainfall (Seubert, 2010), due to upper tropospheric teleconnection centers in the central-northern Mediterranean (modulating subsidence to the east) and northwest of the Tibetan anticyclone (influencing the strength of the Indian monsoon circulation). In addition to these summer aspects of teleconnections, there might also be impacts from Asia affecting subsequent seasons; Alpert et al. (2006) have found that indexes for Indian summer rainfall and Israeli rainfall in the subsequent winter have opposite signs in more than 60% of long-record time series.

A third dynamical system of the tropics is linked with Mediterranean climate variability: the African monsoon system. Within the 30–40°E longitudinal band, Ziv et al. (2004) found a significant correlation during summer between the upward motion at 15–20°N and the downward motion at 30–40°N, indicating a link between the EM and the eastern North Africa driven by the regional Hadley cell. For the western and central MR, an inverse relationship between summer climate and Sahel precipitation has been identified by Baldi et al. (2006), with cooler and wetter Mediterranean conditions concomitant with below-average Sahel rainfall as well as a hotter and dryer Mediterranean summer climate during periods of a strong African monsoon. This pattern seems to be forced by SST anomalies in the Gulf of Guinea (Baldi et al., 2006). A prolonged persistence of the inverse relationship between Sahel rainfall and precipitation in the western and southwestern MR has further been identified for extended periods, including late summer and autumn (Seubert, 2010), mainly due to corresponding variations in the eastward extension of the Azores high.

Many of the teleconnection patterns discussed so far do not work independently of each other, but include considerable interactions and superpositions. Seubert (2010) found a mode representing the combined influence of ENSO and the Indian summer monsoon on rainfall variability in the west/southwestern and east/southeastern MRs during the transition from late summer to early autumn. Increased (decreased) precipitation in these two regions is linked with a weak (strong) Indian summer monsoon in advance of a warm (cold) ENSO event. The author also found a link between the Indian summer monsoon and the EA/WR pattern during summer and early autumn affecting (with negative sign) the corresponding rainfall variability in the northeastern MR.

Furthermore, during spring, a Scandinavian-pattern-like teleconnection mode proves to be linked with SST and rainfall anomalies around the Gulf of Guinea and the tropical Atlantic Ocean (0–20°N), respectively, and this occurs in connection with precipitation anomalies in the western and central MR—a teleconnection

mode that is most pronounced during the decay stage of ENSO events (with negative/positive rainfall anomalies after warm/cold events; see Seubert, 2010). Also, the above-mentioned negative coupling during summer between Sahel rainfall and west/southwestern Mediterranean precipitation seems to be no primary linkage between the African monsoon and Mediterranean circulation dynamics, but rather the result of remote ENSO influences on both systems (Seubert, 2010). The connections between ENSO and NAO with impacts on parts of the MR were mentioned earlier in this section.

This short overview confirms that the MR is influenced by a large number of different teleconnection patterns, including many kinds of covariation, which are often far from being completely understood in terms of circulation dynamics. This also holds for the interactions that are not stable with time, but vary on a decadal timescale, which could be an expression of distinct physical modes or of purely statistical effects.

5.3 Cyclones in the MR and Links to Large-Scale Patterns

This section focuses on the spatiotemporal distribution of cyclone in the Mediterranean, including links with the large-scale patterns discussed earlier. The example of the EM cyclones is used to explain the complex relationship of cyclones, synoptic patterns, and their impact in terms of rainfall and drought. This chapter also addresses extreme cyclones. Effects of cyclones in terms of extremes are discussed in later sections of this chapter.

5.3.1 General Characteristics of Cyclones in the MR

Weather in the extratropical latitudes is largely controlled by the passage of cyclonic systems and their associated fronts, whose occurrence and frequency are to a large extent determined by the distributions of land masses, SST gradients, and the orientation of baroclinic zones. In the MR, cyclones are also one of the main factors determining the weather and climate (Radinovic, 1987). The MR is highly populated by cyclones, especially during winter (Pettersen, 1956; HMSO, 1962; Reiter, 1975; Radinovic, 1987; Campins et al., 2000; Nissen et al., 2010), despite being located south of the global midlatitude climatic belt (Trewartha and Horn, 1980). A particularity here is that the large majority of the cyclones affecting the MR are generated within the Mediterranean basin itself and nearby areas. They develop and evolve within a range of spatial and temporal scales that are intrinsically different from those of extratropical cyclones; they are typically smaller and shallower than north Atlantic systems and have shorter lifetimes (Trigo et al., 1999). Still, they are able to induce extreme precipitation and floods (Buzzi et al., 2005; Homar et al., 2007), wind storms (Nissen et al., 2010), and storm surges (Trigo and Davies, 2002).

A number of identification and tracking methods have been developed or specifically adapted for cyclones in the MR (Alpert et al., 1990a, 2004a; Trigo et al., 1999, 2002a; Maheras et al., 2001; Picornell et al., 2001; Lionello et al., 2002, 2006a,b;

Raible and Blender, 2004; Buzzi et al., 2005; Pinto et al., 2005; Musculus and Jacob, 2005; Trigo, 2006; Bartholy et al., 2009; Flocas et al., 2010; Campins et al., 2011). These studies showed that the representation and quantification of cyclone activity is sensitive to both the choice of data and the method (Trigo, 2006; Raible et al., 2008; Ulbrich et al., 2009). Catalogs of Mediterranean cyclones have been constructed within the framework of the MEDEX and CIRCE projects (http://medex.aemet.uib.es/index.html, http://www.circeproject.eu). Figure 5.4A shows a climatology of cyclones produced from ERA40 data for the whole year, showing distinct areas with strong activity over the Gulf of Genoa and over Cyprus. Clearly evident maxima of cyclone track density are also found over the Iberian Peninsula and over the Sahara.

In the cold season, the Mediterranean basin offers all cyclogenetic factors; being highly baroclinic, warmer than its surroundings, and positioned at the lee of mountain ridges, such as the Atlas ridge in Morocco, the European Alps, and the Taurus ridge in Turkey (HMSO, 1962; Alpert et al., 1990a, 1996; Tafferner and Egger, 1990; Stein and Alpert, 1993; Trigo et al., 1999, 2002a; Lionello et al., 2006a; Flocas et al., 2010; Campins et al., 2010). Figure 5.4B shows cyclogenesis areas of Mediterranean cyclones. Two main cyclogenetic regions are clearly visible in this figure: the lee of the Atlas Mountains (Thorncroft and Flocas, 1997; referred to as Sharav cyclones) and the Gulf of Genoa (Buzzi and Tibaldi, 1978; referred to as Genoa cyclones). The cyclogenetic region in the vicinity of Cyprus (described, for example, by Alpert et al. (1990a) and Ziv et al. (2009)) is not clearly detached from the strong maximum east of the Mediterranean according to the analysis performed in Figure 5.4B. Secondary cyclogenetic areas such as the Aegean Sea (Flocas and Karacostas, 1996; Flocas, 2000), the Sahara, the Iberian Peninsula, southern Italy (Maheras et al., 2002), and the Algerian Sea are not clearly visible as annual maxima in this figure. According to Maheras et al. (2002), the winter Cyprus cyclones are characterized by a remarkably stronger baroclinic character as compared with other MR cyclones.

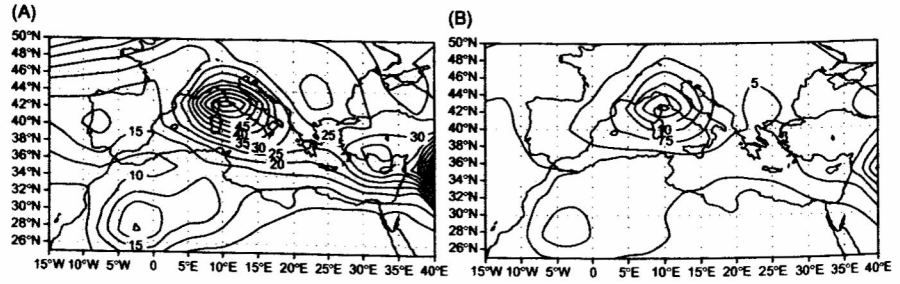

Figure 5.4 (A) Cyclone track density, computed according to Nissen et al. (2010), contour interval 5 events/year/unit area (see caption of Figure 5.8). (B) Cyclogenesis (initial occurrence of identified cyclones), contour interval 2.5 events/year/unit area. Based on Annual ERA40 data for the period 1957–2002.

5.3.2 Seasonal Variations of Cyclones

The regional distribution of Mediterranean cyclones shows a strong seasonal signal, as cyclones are located preferentially in some regions for particular seasons (Figure 5.5). The pattern for summer (JJA) is rather similar to that for spring (MAM), and is in contrast to that for winter (DJF) and autumn (SON), which again resemble each other. Only the maxima in the Gulf of Genoa and partially the maximum over Cyprus are stable throughout the year.

The main features for the summer are the large numbers of cyclones over the Sahara and, to a lesser extent, the Iberian Peninsula/Gulf of Cadiz, the Gulf of Genoa, and the area around Cyprus. The large numbers over land are partly due to the occurrence of heat lows, which owe their genesis to thermal heating over land. Stationary heat lows are often removed from cyclone climatologies (Pinto et al., 2005). Such a procedure was also applied for producing Figures 5.4 and 5.5. However, heat lows partly develop into traveling cyclones in conjunction with southward excursion of midtropospheric troughs (Egger et al., 1995; Thorncroft and Flocas, 1997), thus explaining the Sahara track density maximum.

During autumn, the largest cyclone numbers are located in the Gulf of Genoa and the surrounding seas. During winter, the cyclone maximum is located over the Gulf of Genoa, but other areas, such as the Adriatic, the Tyrrhenian, the Ionian, the Aegean, and the Black Seas and Cyprus feature a large number of cyclones (all sea

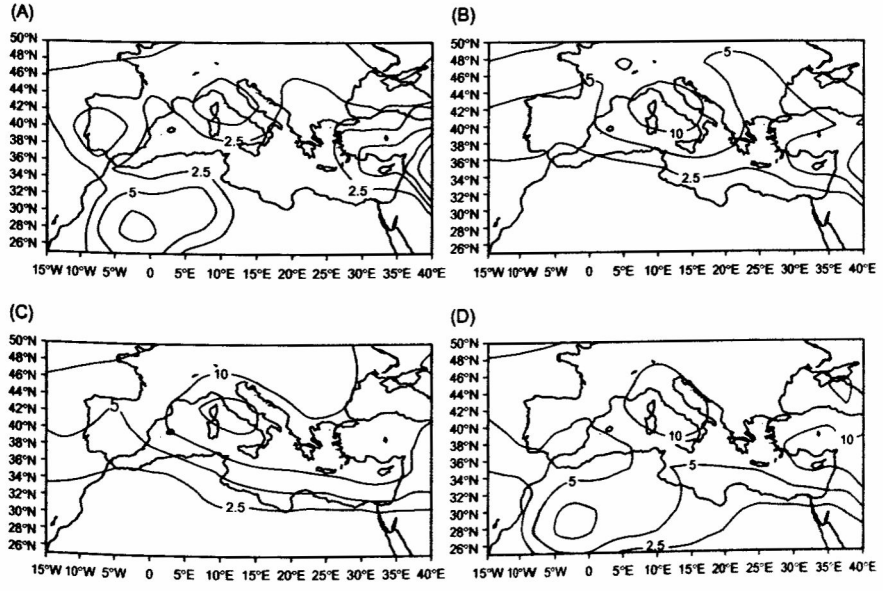

Figure 5.5 Cyclone track density as in Figure 5.4A, but for the (A) summer, (B) autumn, (C) winter, and (D) spring. Contour lines 2.5, 5, 10, 20, and 40.

areas). Winter cyclogenesis is predominantly lee cyclogenesis supported by baroclinic instability (Buzzi and Tibaldi, 1978; Speranza, 1975; also see Section 5.3.3).

5.3.3 Genoa Cyclones and Mechanisms of Cyclone Development

The Gulf of Genoa, located southwest of the Alpine range, is one of the major cyclogenetic areas of the Mediterranean basin. Cyclogenesis occurs there throughout the year, with a maximum in March and April (Campins et al., 2010). Genoa cyclones often develop into deep systems, attaining the highest intensities among Mediterranean cyclones, on average. They generally travel southeastward, affecting the Alpine region, the Italian Peninsula, the Adriatic Sea, and the central and eastern Mediterranean. Genoa cyclones typically originate from lee cyclogenesis on the south side of the east–west oriented Alpine mountain range and are an example of lee cyclones. Strong cyclone growth can occur when a shallow barotropic cyclone induced by orography interacts with an approaching upper tropospheric wave (McGuinley, 1982). The underlying mechanisms are as follows (after McGuinley, 1982; Radinovic, 1986):

1. Development begins when a preexisting upper-air trough approaching the mountain range from the northwest starts to undergo deformation caused by the fact that the cold air mass at lower levels is deflected around the obstacle. At this point, a diffluent upper airflow exists over the region. Through conservation of low-level potential vorticity, a small disturbance in the lee is induced, with anticyclonic circulation in the lower layers and cyclonic circulation in the upper layers (see also Egger, 1995). This is referred to as the "terrain induced barotropic phase" (McGuinley, 1982).

   The deformation of the frontal zone associated with the trough is accompanied by an enhancement of low-level baroclinicity within the domain of the mountain range and the creation of negative vorticity at lower levels in the lee of the mountain, as the readjustment of the circulation takes place. This orographically induced circulation begins to play an active role in the low-level thermal advection. Frontogenetic processes start, forcing upward motion at midlevels over the lee of the mountain barrier (McGuinley, 1982).
2. The rapid development begins as the front passes the mountain region and advection of positive vorticity by the large-scale flow at the upper levels increases rapidly. At this point, the associated upper-air trough often intensifies (McGuinley, 1982). The stretching produces rapid intensification and deepening of the lee cyclone. The indirect circulation previously set up by the mountain changes rapidly to a terrain-enhanced direct circulation, increasing kinetic energy, developing a more baroclinic component. Blocking of the flow at low levels (increasing frontal tilt) and downward motions on the lee slopes of the mountains enhance the direct circulation once the front passes the mountain range. Buzzi and Tibaldi (1978) called this "trigger phase." This phase is the critical moment of the development. Tsidulko and Alpert (2001) pointed out that "phase-locking" between the lower- and higher-level anomalies must occur during this stage. Slight changes in the pattern positions may result in "unlocking," with the potential to stop the further development of the cyclone. This explains why lee cyclogenesis is very sensitive to the phasing of the different factors, and why seemingly favorable conditions do not necessarily result in a lee cyclone (Tsidulko and Alpert, 2001). Coupled with the upper-air trough, the cyclone, which had been quasi-stationary, moves away from the mountain range.

3. As the cyclone moves away from the mountain, it loses the terrain-assisted direct circulation favorable to the formation of kinetic energy. After this phase, the storm must be of sufficient size to grow baroclinically on its own. McGinley and Zupanski (1990) found that the most intense lee cyclones depend more on the strength of the upper-level jet than on the low-level baroclinicity at the frontal zone.

However, as pointed out by Tsidulko and Alpert (2001), there is still no unified theory of lee cyclogenesis, as there is still some lack of agreement on the key dynamic processes. According to Maheras et al. (2002), the conditions and processes leading to their genesis depend on the season. Such differences in the development processes could be due to modifications of the prevailing air mass in which the development takes place. During the winter, the air mass over the western Mediterranean Sea is warmer, more humid, and less stable than over the surrounding land, and it is an important source of energy for the development of the cyclones.

5.3.4 Cyprus Cyclones and Their Related Rains

The synoptic-scale system that is responsible for the vast majority of the annual rainfall in the Levant region is the Cyprus Low (Alpert et al., 1990a; Goldreich, 2003; Ziv et al., 2009). This name is given to the Mediterranean cyclones while they are reaching the eastern part of the Mediterranean basin, not necessarily while located over Cyprus itself. Cyprus Lows are of major importance for rainfall over the EM, and thus their relation to precipitation is briefly discussed in this section as an example for the mechanisms linking cyclones and precipitation. Saaroni et al. (2010) showed that the Cyprus Lows contribute ~80% of the rainfall in Israel in November–March (the part of the season contributing >90% of the annual rainfall) and that the interannual variations in the number of Cyprus Lows explain 50% of the variance in the interannual rainfall variation. Figure 5.6A shows a composite map of extreme precipitation events over Israel, demonstrating the importance of Cyprus Lows in this region.

The characteristic depth of Cyprus cyclones undergoes an annual cycle, with enhanced (negative) geopotential height anomalies at all levels in winter (Maheras et al., 2002). The importance of the intensity (depth) and location of the Cyprus Lows are demonstrated in Figure 5.7 through the average daily rainfall for three synoptic types contributing >50% of the rainfall in Israel. The depth of a cyclone is the pressure difference between its center and its periphery. The distinction between deep and shallow lows (according to Alpert et al., 2004a) is based on a subjective identification done by trained forecasters for a training period of 450 days. For the winter months (December–February), 30% of the Cyprus Lows were deep and the rest shallow. The role of the Cyprus Low intensity can be inferred from comparing the daily rainfall associated with the deep and shallow lows located to the north of Cyprus. The former is about twice as strong, as deeper lows are generally associated with enhanced upslope winds and associated precipitation. The effect of the low's position visible in Figure 5.7 reveals the importance of the moisture transport direction: while the deep low to the north contributes considerably more rainfall in north Israel, the deep low to the east contributes even amounts in north and central Israel,

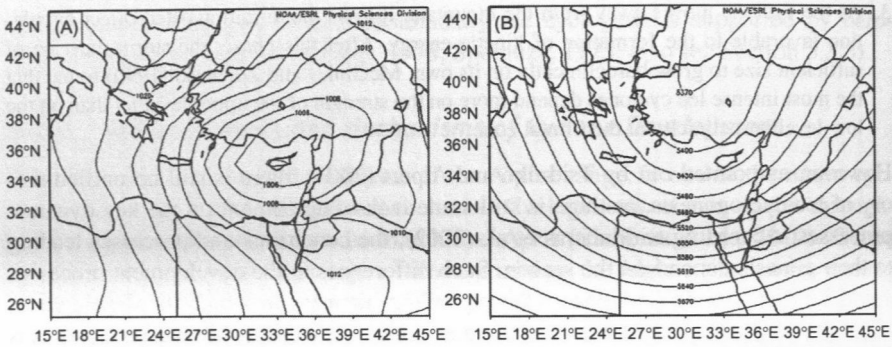

Figure 5.6 Composite map of SLP (A) and 500 hPa geopotential height (B), averaged over 10 days in which intense rainfall, on the order of 50 mm, was observed over north and central Israel, extracted from National Centers for Environmental Prediction (NCEP)-NCAR reanalyzed data (Kalnay et al., 1996; Kistler et al., 2001).

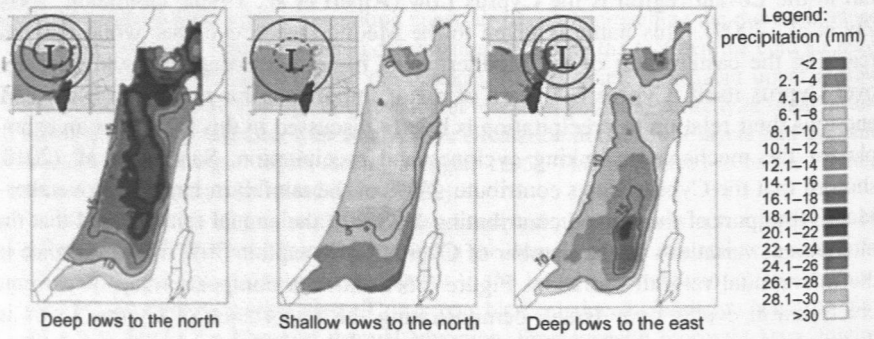

Figure 5.7 Spatial distribution of daily rainfall associated with three types of Cyprus Low (Saaroni et al., 2010).

due to the direct onshore moisture transport to central Israel by the northwesterly winds. Deep lows to the east produce floods in the Negev desert from time to time, which extends south of the region, as shown in Figure 5.7 (Kahana et al., 2002).

In general, the moisture eventually leading to rainfall is not advected with the warm air masses involved in the cyclones. These air masses originate mostly from the arid Saharan Desert (Ziv et al., 2010). The cold air masses, however, while interacting with the relatively warm Mediterranean Sea, become convectively unstable and thus are the major candidates for rain production (Ziv et al., 2010; Harats et al., 2010). The Mediterranean Sea then supplies latent and sensible heat as well as moisture, as shown for Cyprus Lows by Shay-El and Alpert (1991) and Stein and Alpert (1993). While such cold and unstable air masses enter the eastern part of the Mediterranean basin, advected by the westerly winds south of the cyclone core (related to the pressure gradient, Figure 5.6A), they experience upward motion, in

addition to that imparted by the cyclone itself, because of the encounter with the coastline and, later on, with the mountain ridges inland (Alpert and Shafir 1989; Ziv et al., 2009). Cyprus Lows are typically accompanied by pronounced upper-level troughs, as demonstrated in Figure 5.6B, and sometimes cutoff lows (Alpert and Reisin, 1986; Zangvil and Druian, 1990).

5.3.5 North African Cyclones

The North African Cyclones, also called "desert depressions" (Pedgley, 1972) or "Sharav cyclones" (Winstanley, 1972), are a typical spring phenomena for southern Mediterranean countries, such as Libya, Egypt, and Israel (Alpert and Ziv, 1989). The Sharav cyclones form along the Mediterranean southern coastline and at the northern edge of the North African desert (Reiter, 1975; Alpert and Ziv, 1989). Egger et al. (1995) showed that their formation can be considered a secondary lee cyclogenesis of Genoa Lows, which are themselves the result of secondary lee cyclones to European "parent" cyclones (discussed by Romem et al. (2007)).

Their preferred cyclogenetic region is the lee of the Atlas Mountains. The cyclone activity south of the main Mediterranean cyclones' track is explained by the temperature contrast between the Mediterranean Sea and the North African desert to the south. The lag in the seawater response to the annual temperature cycle with respect to the desert causes this contrast to reach its maximum in the spring. During this season they are the most important type of synoptic systems in the EM (Alpert et al., 2004b). They are typically smaller and faster than Mediterranean winter cyclones (Alpert and Ziv, 1989), which makes the duration of the influence of an individual system shorter than a day (compared to several days for the winter Mediterranean cyclones).

Sharav cyclones are typically not associated with frontal rains because of the low moisture content of the warm air mass originating from the Sahara and their small vertical extent, which reduces the vertical velocities (Alpert and Ziv, 1989). Thus, the main phenomena associated with the Sharav Cyclones are extremely hot and dry weather within the warm sector (Winstanley, 1972) and sand and dust storms, especially ahead of and along the cold front (Tantawy, 1969; Alpert and Ziv, 1989; Saaroni et al., 1998).

5.3.6 Explosive Cyclones in the Mediterranean

In the Mediterranean basin, explosive cyclones develop mainly from November to March (Kouroutzoglou et al., 2011). According to the definition of Bergeron (1954) and Sanders and Gyakum (1980), an explosive development (denominated "bomb") is characterized by an unusually large deepening, with rates of at least 1 hPa/h for 24 h for a reference latitude of 60°N. Considering the latitudinal correction suggested by Sanders and Gyakum (1980), cyclones with deepening rates of 20 and 14 hPa/24 h at the northern and southern boundaries, respectively, of the MR should be considered explosive, but different suggestions for thresholds suitable for the MR have been made (Kouroutzoglou et al., 2011). Synoptic climatologies

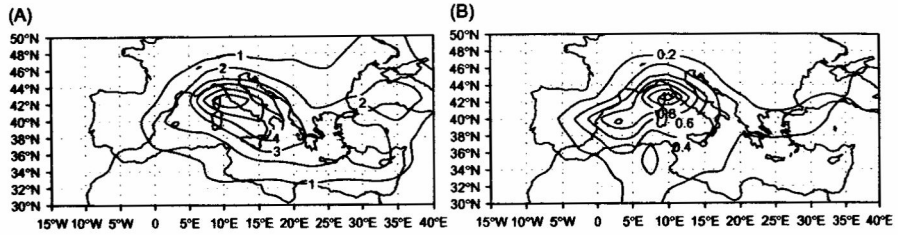

Figure 5.8 Mediterranean bombs: (A) Cyclone track density in tracks per year over unit areas (equal to the area of a square with 1° latitude side length). (B) Cyclogenesis in events per year per unit area. Method based on Kouroutzoglou et al. (2011).

of explosive developments over the Mediterranean have been carried out by Conte (1986) and Conte et al. (1997) and more recently by Kouroutzoglou et al. (2011). In terms of case studies, exceptional cases of Mediterranean bombs were examined by Karacostas and Flocas (1983), Prezerakos and Michaelides (1989), and Lagouvardos et al. (2007).

Figure 5.8 shows the geographical distribution of the density of explosive cyclones in the Mediterranean. The area with the large majority of occurrences is found north of 40°N, with a maximum in the Gulf of Genoa, and it extends southeastward over the Aegean Sea. The western basin clearly dominates, particularly the Gulf of Genoa and the area near the Baleares. However, the bomb cyclones' size and depth are typically larger in the EM than in its western part (Kouroutzoglou et al., 2011).

5.3.7 *Links Between Cyclones and Large-Scale Patterns*

The influence of the NAO, the EA/WR, and the SCAND (see Section 5.2) patterns on cyclones was analyzed by Nissen et al. (2010). Figure 5.9 depicts the difference of the cyclone track density between the positive and the negative phase of the NAO (A), EA/WR (B), and SCAND (C) patterns for the winter. As expected from previous studies (Hurrell and van Loon, 1997; Trigo et al., 2002b), the storm track is intensified and shifted northward during the positive NAO phase (Figure 5.9A), while Mediterranean cyclone activity is enhanced during the negative phase. This signal is significant over the western part of the Mediterranean basin. The EA/WR is of comparable importance for the number of MCs as the NAO. Its positive phase is associated with a reduction of tracks over the northern part of the MR, in particular over central Italy and the Adriatic basin (Figure 5.9B). In contrast, the Levant region is affected by more cyclones during the positive phase of the EA/WR pattern. This is in agreement with studies analyzing precipitation in Israel, which found an increase in precipitation during the positive phase of the EA/WR (Krichak et al., 2002, 2004). A positive phase of SCAND is associated with an increase of the total number of winter cyclones in the western and eastern MR (Figure 5.9C). Comparing positive and negative index values, the affected areas and the track density anomalies are smaller than for the other two patterns.

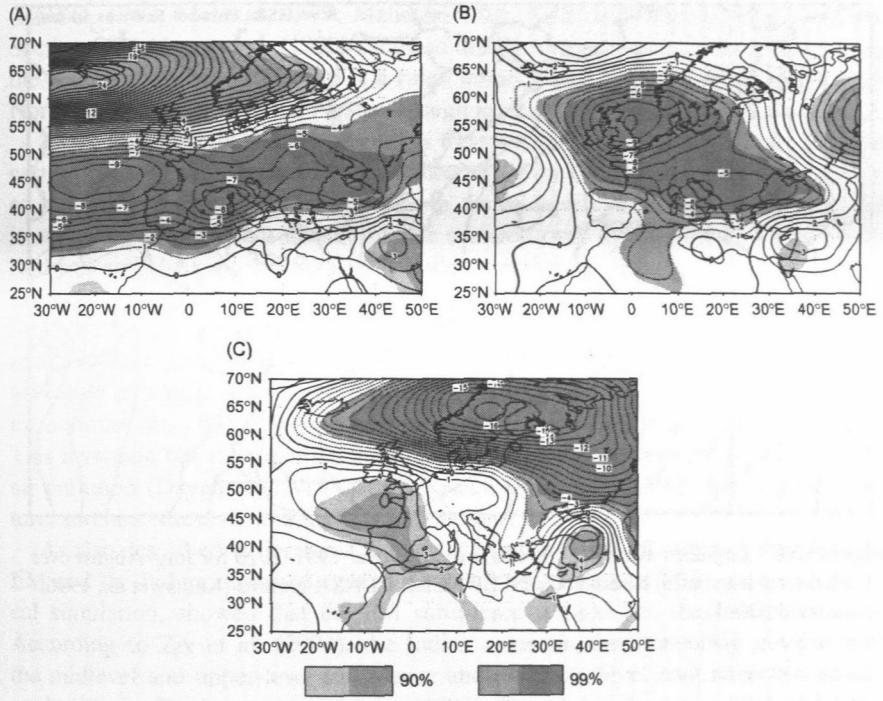

Figure 5.9 Cyclone track density difference between positive and negative index values of: (A) NAO, (B) EA/WR, and (C) SCAND in number of cyclones per extended winter season and per unit area (see caption of Figure 5.8).
Source: Figure taken from Nissen et al. (2010).

5.3.8 Synoptic Patterns in the EM

The summer season over the EM is characterized by minor interdiurnal variations in various climatic variables, such as temperature, pressure, and wind. The monotonic nature of this season is explained by the relatively persistent synoptic conditions (Ziv et al., 2004). They are thus considered in some more detail in the present section.

The lower levels are dominated by a trough extending from the Persian Gulf through southern Turkey into the Aegean Sea, known as the Persian Trough (Figure 5.10). The background for the Persian Trough formation is the large-scale northerly winds prevailing over the EM in the summer due to the combination of the Indian monsoon to the east and the Azores high to the west. The Persian Trough develops as a result of the topographic effect of the mountain ridges extending from Iran down to Asia Minor (the Taurus Mountains) on the prevailing northerly winds. It persists over the EM during the entire summer—i.e., mid-June to mid-September (Figure 5.11). The Persian Trough induces persistent north-to-northwesterly winds over the EM, known as the "Etesian winds," which cause high sea levels, especially in the Aegean

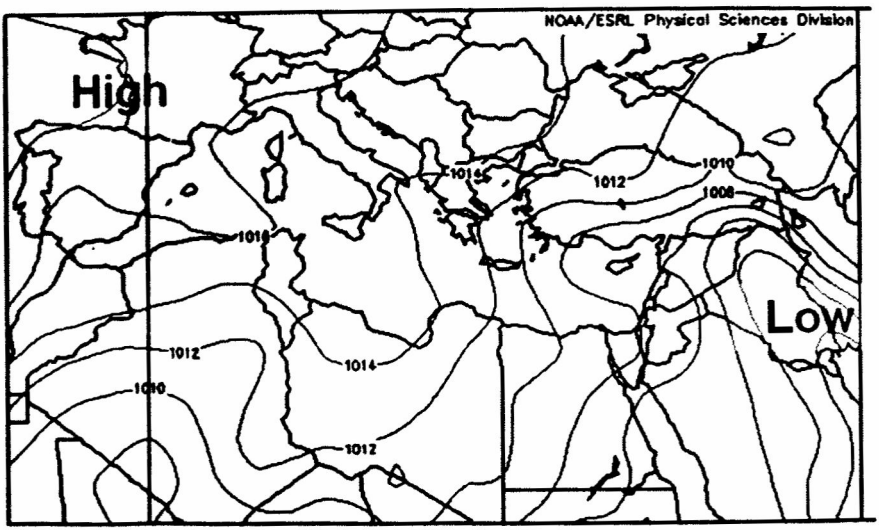

Figure 5.10 Long-term mean SLP (in hPa) averaged over 1981–2010 for July–August over the Mediterranean basin, based on the NCEP/NCAR CDAS-1 archive (Kalnay et al., 1996; Kistler et al., 2001).

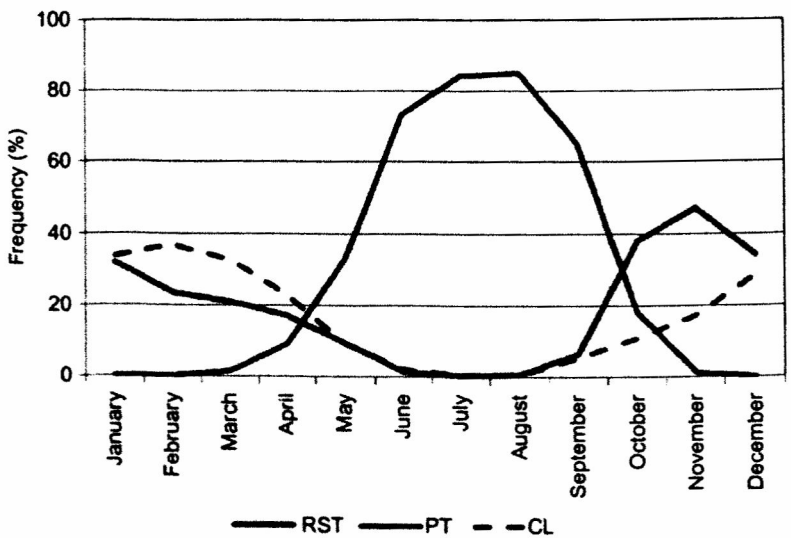

Figure 5.11 Climatological annual cycle of the dominant EM synoptic systems. The figure shows the monthly frequency (%) of each synoptic system. The black line represents the Persian Trough, the dashed line Cyprus Lows ("winter low"), and the gray line the Red Sea Trough (RST).

(HMSO, 1962; Metaxas, 1977; Maheras, 1980; Bitan and Saaroni, 1992; see also Section 5.5). Alpert et al. (1990b) showed that the main dynamic feature dominating the southeastern Mediterranean is a ridge linked to the Azores anticyclone through North Africa, rather than the Persian Trough located to the north.

At the lower levels, the Etesian winds transport moist and relatively cool air to the eastern coast of the Mediterranean as they pass over the Mediterranean Sea (Alpert et al., 1990b; Saaroni and Ziv, 2000). In the midlevels and higher levels, the EM is subjected to persistent air subsidence centered over Crete (Alpert et al., 1990b; Rodwell and Hoskins, 1996). This subsidence makes the EM the area with the lowest specific humidity in the northern hemisphere for July–August at the 300–500 hPa level, preventing rain over the region during this season (Saaroni and Ziv, 2000; Ziv et al., 2004). The combination of midtropospheric subsidence and lower-level cool advection enhances the marine inversion, which prevails over the Levant region in the summer (at ~700–900 m above sea level in Israel (Dayan and Rodnizki, 1999). This inversion has far-reaching environmental implications because of its effects on air pollution (Dayan et al., 1988, 2002; Koch and Dayan, 1992), lower-level moisture, and heat-stress conditions (Ziv and Saaroni, 2011).

As also described in Section 5.2, there is a link between the summer regime in the EM and the Indian monsoon system. Rodwell and Hoskins (1996), using a numerical simulation, showed that the EM subsidence is linked to the Indian monsoon. According to Ziv et al. (2004), the Indian monsoon simultaneously governs both the midlevel and upper-level subsidence and the lower-level cool advection associated with the Etesian winds. Webster (1994) showed (for the years 1985 and 1987) a circulation that connects the EM with the Asian monsoon; air ascends at the monsoon region and descends over the EM and thus warms and dries the upper levels. Ziv et al. (2004) showed a circulation connecting these two regions through vertical-meridional and isentropic cross-sections based on long-term averaged winds for July–August.

In the EM, there is also a significant synoptic feature related to the African monsoon, the Red Sea Trough. A pressure gradient is usually observed between North Africa, which is influenced by a monsoon trough (with a normal position for October 15–20°N over the heated continental interiors of central and East Africa; Barry and Chorley, 1998), and the MR. However, low-pressure troughs may extend from the African monsoon toward the Mediterranean (Ziv, 2001; Dayan et al., 2001). The Red Sea Trough is a pronounced example of such a trough, extending from East Africa or Saudi Arabia toward the EM (Ashbel, 1938; Kahana et al., 2002). Its prevalence in the fall season is expressed in the long-term mean SLP for October–November (Figure 5.12). It can be attributed to the Lee effect imparted by the continuous mountain ridges east of the Red Sea, which extend from southeast to northwest.

The annual frequency of the Red Sea Trough system in the EM is 19% of the days (Alpert et al., 2004a; see Figure 5.11) with a maximum in autumn and significant occurrence during the winter (Alpert et al., 2004b; see Figure 5.11). Surface wind direction and consequently the weather conditions in the Levant region are highly dependent on the position of the Red Sea Trough axis (Saaroni et al., 1998; Tsvieli and Zangvil, 2005). Alpert et al. (2004a) used its location with respect to the eastern

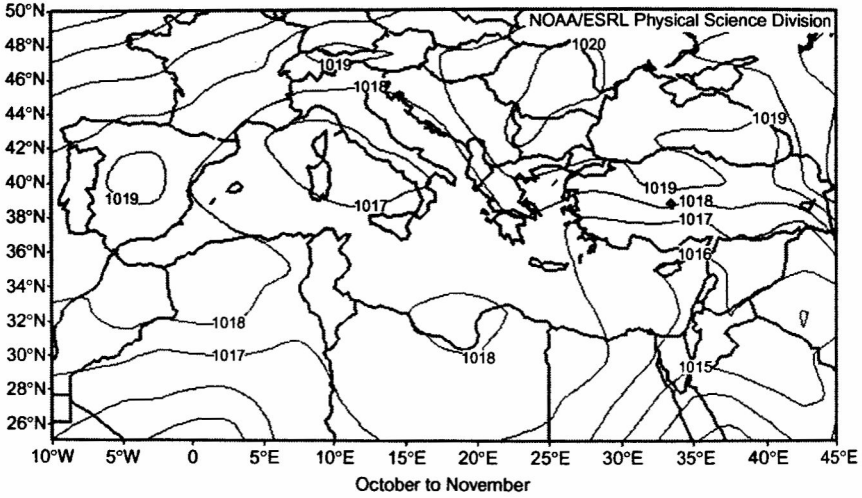

Figure 5.12 Long-term mean SLP (in hPa) averaged over 1981–2010 for October–November over the Mediterranean basin, based on the NCEP/NCAR CDAS-1 archive (Kalnay et al., 1996; Kistler et al., 2001). Note the signature of the Red Sea Trough over the Levant.

coast of the Mediterranean for categorizing the three types of Red Sea Trough—i.e., with eastern, central, and western axes. The eastern position is associated with northerly winds over the eastern coast of the Mediterranean (the Levant region). This, together with the dominance of the sea breeze (typical to warm climates), implies onshore moist advection with low cloudiness. When the Red Sea Trough has a western axis, the winds are southeasterly, implying hot and dry conditions. When the axis is central, the weather conditions are highly variable according to the geometry of the trough axis with respect to the pertinent location along the EM coastline. In many cases, sand storms develop under the influence of the southeasterly winds over the sandy basins in Saudi Arabia and Iraq, and the dust is transported westward, to the Levant.

The Red Sea Trough is a lower-level system. In most events, the upper levels are characterized by westerly winds or even anticyclonic flow. The combination of the absence of upper-level dynamic ascent and dry airflow at the lower levels prevents the Red Sea Trough from being a rainy system (Dayan et al., 2001; Ziv et al., 2005a,b). However, the above-normal temperatures at the lower levels produce conditional instability. At times, a sharp upper-level trough of midlatitude origin, or a cutoff cyclone, develops over the Nile delta. The implied midlevel southerly winds transport tropical moisture to the Levant, and intense tropical-like thunderstorms occur—with extreme rain rates, hail, and floods, especially over Egypt, Saudi Arabia, south Israel, and Jordan (Ashbel, 1938; El Fandy, 1948; Dayan et al., 2001; Ziv et al., 2005a,b). This type of Red Sea Trough is named "active" and is accounting for the major floods that occurred in the Negev desert of Israel (Kahana et al., 2002).

The active Red Sea Trough is a typical example of tropical/extratropical interaction in which elements from a variety of climatic regimes, the African monsoon, the subtropical jet, and midlatitude systems are involved. They are relevant for the moisture sources as discussed in Chapter 6. With regard to the dynamics involved, Krichak and Alpert (1998) considered the subtropical jet to be a key factor and Dayan et al. (2001) concentrated on the role of the upper-level trough. The enhanced southwesterly flow at the midlevels ahead of the trough, while transporting moisture from western equatorial Africa to the EM, enhanced upward air motion implied by the divergence at that level. Dayan et al. (2001) also considered the contribution of the overlapping of two divergence zones associated with polar and subtropical jets as the background for an explosive cyclogenesis, similar to the type suggested by Uccellini and Kocin (1987).

Several studies (Dayan et al., 2001; Kahana et al., 2002; Ziv et al., 2005a,b) showed that prior to the evolution of an active Red Sea Trough, a continued abnormal southerly flow prevailed over eastern Africa. This served as an "incubation period," promoting the advection of tropical air masses toward the EM and the expansion of the lower-level trough.

5.4 Temperature and Temperature Extremes

This section considers temperatures and their extremes, with a special focus on recent observed trends. Both mean temperatures and temperature extremes (e.g., tropical nights and heat waves) are discussed, mentioning the importance of regional and local mechanisms and of large-scale atmospheric circulation anomaly patterns (such as the NAO or blocking features). Remote factors such as ENSO and Asian monsoon anomalies also play a role in producing regional temperature anomalies in the MR. The effects are partly dependent on the season considered.

5.4.1 *Mean Temperature Trends and Large-Scale Atmospheric Circulation Regimes*

Temperatures in the Mediterranean are characterized by high spatial complexity and a pronounced seasonal cycle, and they are influenced by large-scale atmospheric circulation, land–sea interactions, and local processes (Xoplaki et al., 2003; Trigo et al., 2006).

In the past six decades, an overall warming tendency has been reported (Brunet et al., 2007a; Brunetti et al., 2009; Kafle and Bruins, 2009; Toreti, 2010; Toreti et al., 2010a). The recent upward tendency is particularly pronounced in summer, while several locations do not show a significant trend in winter (El Kenawy et al., 2009; Toreti, 2010; Toreti et al., 2010a), although on a centennial timescale, trends are highly significant in all seasons (Brunetti et al., 2009). It is important to highlight that the recent trend started in the late 1970s–early 1980s in the western Mediterranean (Miranda and Tomé, 2009; Toreti et al., 2010a) and only in the late 1980s–early 1990s in the EM (Miranda and Tomé, 2009; Tayanç et al., 2009).

The identified temperature trend in the twentieth century has been connected with a reorganization of atmospheric regimes (Corti et al., 1999; Philipp et al., 2007)

attributed to a combination of greenhouse gas forcing and internal/natural variability (Corti et al., 1999; Osborn, 2004). Extratropical tropospheric circulation has often been investigated by assuming the paradigm of multiple regimes, although the hypothesis is still debated (Stephenson et al., 2004; Christiansen, 2009). The exact number of regimes is also still controversial; two to four winter regimes have been identified (Michelangeli et al., 1995; Casty et al., 2005a,b; Hannachi, 2010) and linked to the position of the North Atlantic eddy-driven jetstream (Woollings et al., 2010, and references therein). The four regimes that recur in the analysis of winter in northern hemisphere atmospheric circulation and temperature are the positive and negative phases of the NAO, the blocking regime, and the Atlantic ridge (Goubanova et al., 2010). The fingerprint of the positive and negative phases of NAO on mean temperature (Figure 5.13) is apparent across the central/northern Euro-Mediterranean region. As outlined by Pozo-Vázquez et al. (2001), the relation between NAO and temperature is not linear in many European areas, where a stronger temperature response is identifiable during the positive than during the negative NAO phase (Iberian Peninsula and central Europe).

According to Maheras et al. (1999), the geographical distribution of high winter (and also in spring and autumn) temperatures over the Mediterranean is associated with a negative SLP anomaly to the west of the Mediterranean basin, above which a region with relatively high-pressure values may be found. This constellation produces southwesterly flow into the western Mediterranean. It may also allow warmer air from North Africa to influence eastern parts of the basin. On the contrary, particularly cold months occur in winter, when a northerly component to the flow into the Mediterranean is produced. Some of the most pronounced basinwide cold events, in autumn as well as in winter, are associated with positive SLP anomalies to the west or northwest of the British Isles, while lower-than-normal SLPs are located southward. This pressure

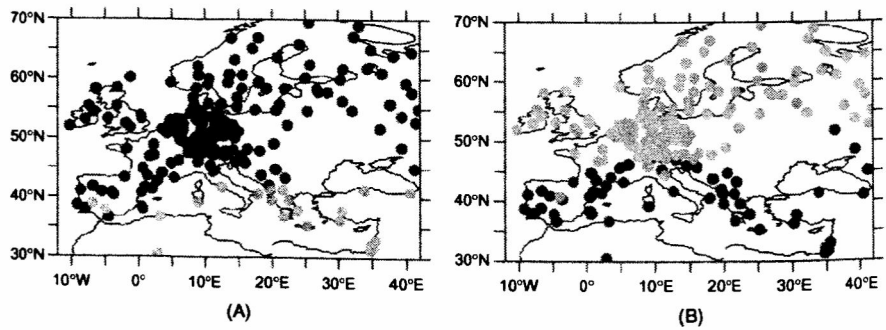

Figure 5.13 Weather regimes favoring the occurrence of warm (A) and cold (B) temperatures. Red is associated with the positive NAO, yellow with the negative NAO, green with the Atlantic ridge, and blue with the blocking regime. (For interpretation of the references to color in this figure legend, the reader is referred to the web version of this book.)
Source: Figure reprinted from Goubanova et al. (2010), with the permission of the American Meteorological Society.

distribution is associated with a strong negative phase of the NAO (Maheras et al., 1999) or a strong negative phase of the EM pattern (Hatzaki et al., 2007).

The blocking regime is characterized by a strong positive anomaly centered between the Scandinavian Peninsula and the British Isles, with a persistence of ~10 days (Pavan et al., 2000; Scherrer et al., 2006; Croci-Maspoli et al., 2007). As shown in Figure 5.13, the blocking regime influences especially northeastern Europe, which becomes warmer, and the EM, which becomes colder. The Atlantic ridge and the connected anticyclonic circulation over the North Atlantic lead to colder temperatures in the western and central Mediterranean.

Mediterranean summer temperatures are connected with blocking conditions and an east–west dipole over the Euro-Atlantic sector (Xoplaki et al., 2003). Weak large-scale westerly flow combined with persistent anticyclonic regimes over the MR are associated with local heating anomalies (Carril et al., 2008). Furthermore, the heating of the Mediterranean Sea amplifies anticyclonic conditions (Feudale and Shukla, 2007). Seneviratne et al. (2006), Vautard et al. (2007), and Zampieri et al. (2009) discussed the necessity of considering the effect of winter drought and dry soil during late spring/early summer in southern Europe for the establishment of hot summers. In general, it is worth pointing out that atmospheric regimes cannot fully explain the winter temperature variability (Yiou et al., 2007) and other important factors (e.g., land–atmosphere interaction, snow-albedo feedback; van den Besselaar et al., 2010; Luterbacher et al., 2007) have to be taken into consideration.

5.4.2 Extreme Temperature and Large-Scale Atmospheric Circulation

In recent years, extreme temperatures have been investigated mainly through the use of indexes (based on percentiles and fixed thresholds; Klein Tank and Zwiers, 2009) and applying an Extreme Value Theory approach (Coles, 2001). An upward trend in the intensity of Mediterranean summer extremes has been identified by several studies (Klein Tank and Können, 2003; Kostopoulou and Jones, 2005; Moberg et al., 2006). Following the mean temperature behavior, Toreti and Desiato (2008) have reported an increase in the number of tropical nights in Italy since the late 1970s–early 1980s. Moreover, Simolo et al. (2010) have pointed out that the warming trend of moderate extremes in Italy, mostly originating from the warm season, is linked to a rigid shift of the density function. On the Iberian Peninsula after the mid-1970s, a significant increase in the duration of warm spells associated with more warm days/nights and a decrease of cold days/nights has been reported (Prieto et al., 2004; Brunet et al., 2007b; Rodríguez-Puebla et al., 2010). Nogaj et al. (2006) applied a Generalized Pareto model to the North Atlantic/MR and have revealed regional increases in frequency and amplitude of hot summer events. Also, in Greece, an increase of warm and tropical nights, especially after the mid-1980s, has been noted by Kioutsioukis et al. (2010). Finally, significant increases in the intensity, length, and number of heat waves have been pointed out for the western and eastern MR by Della-Marta et al. (2007a) and Kuglitsch et al. (2010), respectively. As shown in Figure 5.14, warm winter extremes are associated mainly with the two NAO phases, while cold winter extremes are associated with a negative NAO

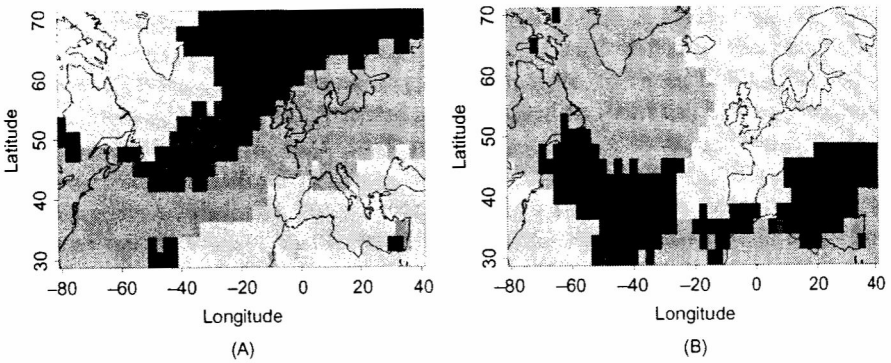

Figure 5.14. Weather regimes associated with warm extremes (A) and cold extremes (B). Red is associated with the Atlantic ridge, green with the negative NAO, orange with the positive NAO, and blue with the blocking regime. (For interpretation of the references to color in this figure legend, the reader is referred to the web version of this book.)
Source: Adapted from Yiou and Nogaj (2004), published at Geophysical Research Letters.

and the blocking regime (Yiou and Nogaj, 2004; Scaife et al., 2008). As outlined by Prieto et al. (2004) for Spanish stations, synoptic processes provide the necessary conditions (e.g., cold flow), but they do not completely determine the occurrence of extreme cold events. The influence of other factors, namely, the extent of snow cover and the northeastern Atlantic SST, has been highlighted by van den Besselaar et al. (2010) and Cattiaux et al. (2011), who note that several factors and feedbacks (in particular associated with snow cover and soil moisture) must be taken into account to explain these trends. As for summer temperature extremes, the blocking regime and the presence of an anomalous trough over the North Atlantic with associated anticyclonic conditions over the Euro-Mediterranean region lead to the development of extreme hot events and heat waves in this region (Cassou et al., 2005; Della-Marta et al., 2007b; Carril et al., 2008). Heat waves have also been related to a persistent northward shift of the Atlantic Intertropical Convergence Zone (Cassou et al., 2005; Carril et al., 2008). Finally, the contributions of the Atlantic and Mediterranean SST forcing and land–atmosphere interactions to the occurrence of extreme events, their intensity, and persistence need to be taken into consideration (Della-Marta et al., 2007b; Fischer et al., 2007).

5.5 Precipitation Extremes

This section describes the extreme values of precipitation in the Mediterranean. Extremes are an aspect of Mediterranean precipitation with very important effects. In general, Trenberth et al. (2007) and Beniston (2007) point to the fact that climate change is and may be mostly perceived through the impacts of extreme events. In the

Euro-Mediterranean region from 1970 to 2006, Barredo (2009) reported 122 extreme flood events with total losses of 140 billion US dollars (2006 normalized value). In 2009, winter storm Klaus (Liberato et al., 2011; with associated heavy rainfall) caused overall losses of 5.1 billion US dollars in France and Spain (Munich, 2010).

In the past five or six decades in the MR, extreme precipitation events do not show a homogeneous tendency. On the Iberian Peninsula, several studies (Moberg et al., 2006; Brunet et al., 2007b; Rodrigo and Trigo, 2007) have pointed out this lack of spatial coherence. However, Alpert et al. (2002) reported a highly significant increase in torrential rainfall (>128 mm/day) and a decrease in moderate precipitation (between 16 and 64 mm/day) in Spain. Moreover, Rodrigo (2010) identified in all seasons an increase (decrease) of the probability of daily precipitation below (above) the 5th (95th) percentile, and López-Moreno et al. (2010) found a decrease in the annual number of days with precipitation greater than the 90th percentile in 49% of the series analyzed in the northeastern part of the Iberian Peninsula, with most remaining stations showing no significant trend (46%). On the Italian Peninsula, Alpert et al. (2002) estimated, on one hand, significant increases in heavy and torrential rainfall (>64 mm) and, on the other hand, a decrease of light-to-moderate precipitation (4–32 mm). Kostopoulou and Jones (2005) identified an increase in the annual number of events with precipitation ≥10 mm, although Norrant and Douguédroit (2006) reported a decrease (3 days/50 yr) in the winter season associated with a negative trend in the amount of precipitation due to these events (74.2 mm/50 yr). With regard to the EM, a significant decreasing trend affects the annual number of events with daily precipitation ≥10 mm (Kostopoulou and Jones, 2005; Kioutsioukis et al., 2010). In winter, the amount of precipitation due to these events also exhibits a negative trend (74.2 and 115.1 mm/50 yr for Greece and the rest of the region, respectively; Norrant and Douguédroit, 2006), while the amount of precipitation due to events above the 95th percentile shows a positive trend in Greece (Norrant and Douguédroit, 2006).

Applying a procedure based on recently developed methods in the Extreme Value Theory, Toreti (2010) provided a statistical characterization of extreme extended winter (October–March) precipitation at 286 stations in the region by deriving return levels and associated uncertainties. As shown in Figure I.10 in the Introduction, the stations with the highest return level are located at coastal sites (e.g., the Gulfs of Genoa and Lion). Moreover, for 7 (83) of these stations, the respective precipitation values are greater than (in the range) 200 mm (100–200 mm).

The development of extreme precipitation events in the MR cannot be attributed to a single factor, but it is caused by the interaction and/or combination of different elements acting at the local and large scales. Among these factors, it is worth citing the role of the Mediterranean SST, moisture fluxes from the North Atlantic, and the orographic forcing provided by the Alps, the Pyrenees, and the Atlas mountains. As for the large-scale circulation, using a subset of 20 coastal stations from the Mediterranean daily precipitation series, Toreti et al. (2010b) identified three spatial patterns of Z500 (SLP) anomalies associated with these events (separately for the western and the EM), characterized by relevant features significantly different from patterns associated with dry days. Figure 5.15 shows an example of the identified

Z500 anomalies for the western and EM. This analysis indicates an association of the events in the western Mediterranean with conditions favoring intense Genoa cyclones (refer to Section 5.3.3), while the EM pattern is associated with Cyprus Lows (Section 5.3.4). Several studies (Jansa et al., 2001; Duffourg and Ducrocq, 2011) discuss the relation of extreme rainfall events and the presence of cyclones modulating local humidity advection. In detail, the association of intense precipitation events with the position and intensity of the cyclones can depend on the location of the extreme event and the characteristics of its environment, in particular with respect to orography (Reale and Lionello, 2011, personal communication).

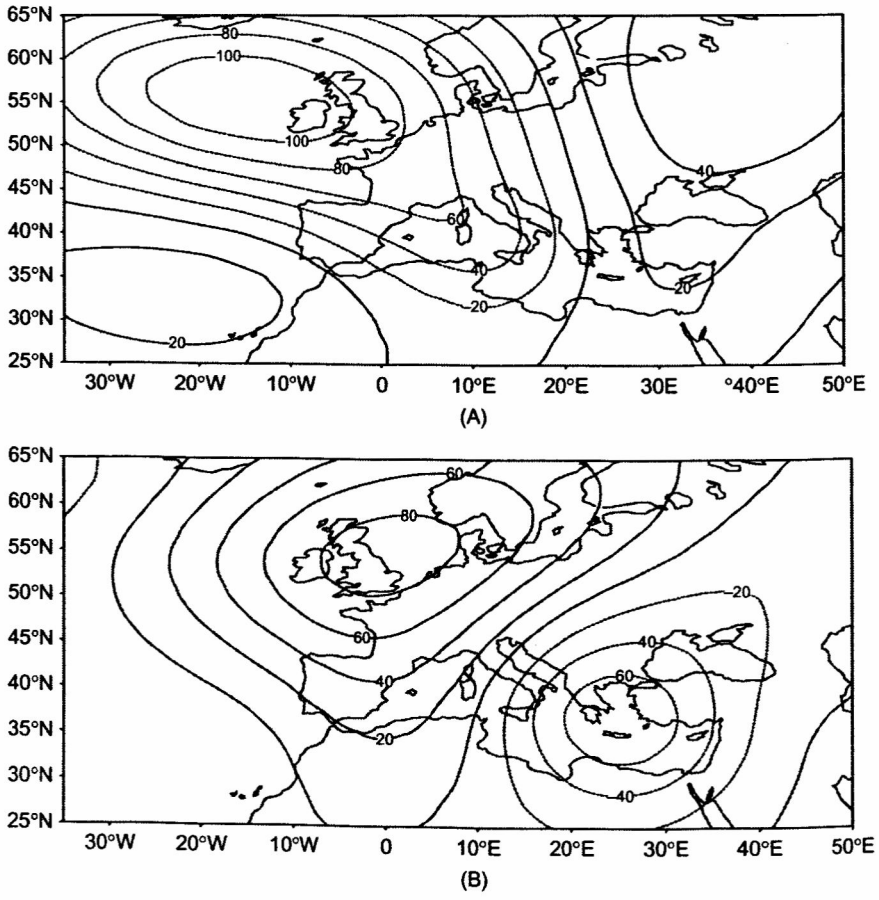

Figure 5.15. Anomalies of geopotential height at 500 hPa associated with extreme precipitation events in the western (A) and eastern (B) Mediterranean.
Source: Toreti et al. (2010b).

5.6 Wind and Wind Extremes: Wind Storms, Dust Storms, and Storm Surges

5.6.1 Extreme Winds and Wind Storms in the Mediterranean

Extreme wind events in the Mediterranean basin develop for three main reasons. First, extreme wind speeds are a consequence of organized structures related to the genesis of extreme surface-pressure anomalies originating from thermal (local) causes, baroclinic disturbances, or even from cooperation between larger-scale baroclinic and smaller-scale barotropic instability (Reale and Atlas, 2001). Second, high wind speeds develop in mesoscale convective situations. Under the influence of organized deep convection, large amounts of latent heat are released, inducing higher midtropospheric upward wind speeds in an unstable environment, thus leading to increased low-level convergence and high turbulent structures, including surface-gust wind speeds of about 50 m/s in mesoscale convective cells (Lopez, 2005). Third, extreme wind can be forced by orographic effects in combination with typical local weather situations. Figure 5.16 (based on regional climate model simulations with the COSMO Climate Limited-area Model (CCLM); Jaeger et al., 2008) shows where the potential for the occurrence of high wind speeds is substantially increased as compared with the rest of the Mediterranean basin: in the Gulf of Lions (Mistral), in the Aegean Sea, and in various smaller areas of the Tyrrhenian, Ionian, and Adriatic Seas and the Levantine basin (Zecchetto and De Biasio, 2007; Belušić and Guttler, 2010; Section 5.6.2).

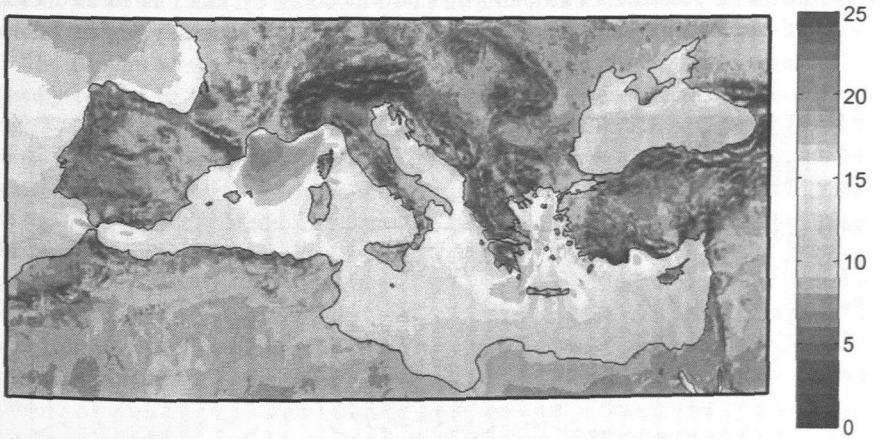

Figure 5.16 Ninety-eighth percentile of the surface (10 m) wind speed as simulated with a high-resolution (7 km) regional climate model (CCLM) for the period from January 1, 2004, to December 31, 2006, forced by the operational global numerical prediction model of the Deutscher Wetterdienst. Units are meters per second. Simulations performed by A. Will (BTU Cottbus).
Source: From Becker (2010).

A comprehensive assessment of the frequency distribution of extreme winds forced by convective activity is difficult and beyond the actual spatial coverage of observation techniques (especially over land) and will not be further described in detail here. Although extreme relevant local impacts might result from the occurrence of these local convective storms, a specific interest lies in the assessment of broader-scale organized extreme wind events forced by low-pressure systems. Leckebusch et al. (2008) developed an objective method to identify and track coherent clusters of high wind speeds relative to the regional background wind climatology. The approach tracks clusters of grid boxes where the wind speed exceeds the local 98th percentile, keeping only spatial and temporal coherent events (Leckebusch et al., 2008). The technique was used by Nissen et al. (2010) to relate the tracks of extreme wind events from the Mediterranean to the responsible cyclone systems and to investigate the influence of large-scale teleconnection patterns on organized extreme wind events in the Mediterranean.

Based on this approach, regions with enhanced frequency of extreme winds can be identified. The most active region is found south of the Ligurian Sea, strongly related to cyclones occurring over the Gulf of Genoa. A secondary maximum is identified over the EM centered south of Cyprus. A third maximum is revealed to the southeast of Sicily (Figure 5.17). The wind-storm activity in Figure 5.17 is displayed in terms of track density, which is the number of tracks that cross a region; it is given here per winter season.

The distribution of cyclones associated with the extreme Mediterranean wind events reflects the wind track density pattern with maximum numbers over a band from the Gulf of Genoa via Sicily toward the Cyprus region in the EM. It is also revealed that a secondary maximum of storm-inducing cyclones is located over the Northeast Atlantic near the European continent, with generally higher values

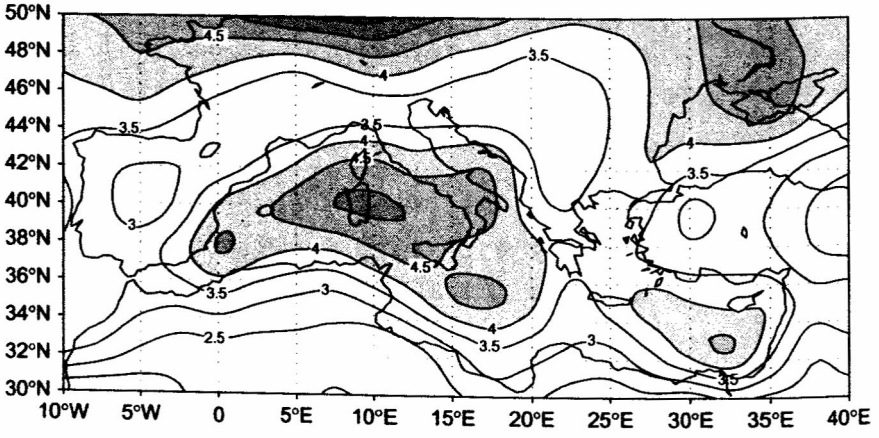

Figure 5.17 Wind-storm-track density for winter (October–March) based on 45 years of ERA40. Units are numbers of events per winter per unit area (see caption for Figure 5.8). *Source*: Based on Nissen et al. (2010).

for the Laplacian of pressure (a measure for cyclone intensity) than those in the Mediterranean basin. In the southern part of the Mediterranean basin, the number of cyclones causing wind storms is rather low and the systems are mostly weak.

The variability of the occurrence of organized extreme wind-speed events is influenced by large-scale variability modes. The difference between positive and negative NAO situations with respect to wind events over the Ligurian Sea and south of Greece is about 50% of the mean annual number of wind storms in these regions, with enhanced numbers of wind storms in NAO-positive phases. The influence of the EA/WR pattern is smaller and different for the western and eastern parts of the Mediterranean basin. Thus, a clear positive change is found over the eastern basin, while over the western basin the positive phase of the EAWR pattern will lead to negative anomalies in the frequency of extreme wind storms. The influence of the SCAND pattern is relatively weak (Nissen et al., 2010).

5.6.2 Local Winds and Wind Extremes

Mediterranean winds are significantly influenced by orography. Orographically generated winds can be thought of as persistent winds that would change their nature, strength, and extent if the specific orographic features were removed. However, they are always related to a certain synoptic situation that provides the primary pressure gradient. This requires the existence of a surface low-pressure system, an anticyclone, and/or a front over the MR or farther away (Burlando, 2009). Even when winds are mainly the consequence of the primary pressure gradient, the airflow is usually modified by local terrain or land–sea contrast to produce the final local wind system (Zecchetto and De Biasio, 2007), which, if climatologically persistent and of sufficient strength, usually bears a specific name for the region.

The *Etesian* winds are a large-scale flow system over the Mediterranean that is usually related to the summer and autumn pressure gradient between the Azores high and the Persian low (Ziv et al., 2004; see also Section 5.3.8). However, on their south-to-southeastward path, they may impinge on mountains or other orographical features (Kotroni et al., 2001; Pasarić et al., 2009), or they may be superimposed on the local sea–land breeze circulation (Klaić et al., 2009). The latter is frequently the case over the Adriatic (Pandžić and Likso, 2005), with the resulting summer local *Maestro* wind (called "Maestral" locally). A similar situation occurs with the south-to-southeasterly *Sirocco* wind, which usually appears as a result of a cyclone over North Africa (Saaroni et al., 1998). While blowing over the wider area, it interacts with smaller- or larger-scale terrain features. The northwest–southeast-oriented Dinaric Alps along the eastern Adriatic coast represent a barrier that, together with the Apennines on the west side, confines the Sirocco airflow to the Adriatic basin. Consequently, the wind is channeled and thereby attains higher speeds and results in a persistent southeasterly wind direction along the Adriatic. These conditions are responsible for storm surges at the northern Adriatic coast, with Venice being the most prominent example of a vulnerable location. It should be noted that the Adriatic Sirocco (also called "Jugo" locally) is not necessarily related to the larger-scale Mediterranean Sirocco, but it may be generated locally by a cyclone northwest of

the Adriatic (e.g., the Genoa cyclone) and/or an anticyclone above the Mediterranean (Pasarić et al., 2007).

However, these winds cannot be considered to be orographically generated airflows that would fit the first category of winds. The most prominent feature of the terrain-generated winds is deducible from looking at the terrain itself—it is hardly regular and homogeneous. The three-dimensional interaction of the impinging airflow with the orography results in a superposition of various dynamical mechanisms that create a local wind system and in a number of specific effects that characterize its behavior. An example of such winds is the *Bora* (also called "Bura" locally), a northeasterly downslope wind across the east Adriatic coast generated by the airflow over the Dinaric Alps. It may appear as a cloudy system that is related to a cyclone southwest of the affected region ("Dark Bora"), or as a clear-sky Bora, whose dominant forcing comes from an anticyclone to the north or northeast. Sometimes it is related to a cold front passing above the area. Each of these synoptic situations ensures a supply of northeasterly cold air impinging on the Dinaric Alps. Several factors influence the response of the system and the final wind configuration. The most important are the mountain height, width, and asymmetry and the vertical structure of the incoming wind speed, direction, temperature, and humidity. In a two-dimensional simplified perspective, the main structure of Bora may be regarded as a hydraulic-like flow. With this view, the surface flow becomes decoupled from upper-level flow above the mountain lee and the energy of the jetlike flow—i.e., the Bora itself—is confined to low levels by mountain wave breaking and/or a temperature inversion, both occurring at heights close to the mountain top. This low-level shooting flow typically ends through dissipation in a hydraulic jump, after which the airflow continues relatively unperturbed. In reality, the three-dimensional effects, such as those caused by the existence of mountain gaps and peaks, significantly influence the Bora wind pattern. Therefore, the final Bora structure is a combination of a downslope windstorm and a gap wind, although it seems that for strong to severe Bora, the downslope component is dominant. With the Bora maxima related to mountain gaps and the minima related to mountain peaks, the typical Bora signature is seen as a sequence of interchanging jets and wakes along the eastern Adriatic spreading toward the southwest. Mean wind speeds during severe Bora events may surpass 30 m/s, with wind gusts being about twice the mean wind speed (the strongest recorded gust was 69 m/s). With such high wind speeds, Bora significantly influences the entire east Adriatic coast, specifically the sea and road traffic. The air–sea interaction during Bora has been intensively studied, particularly in the past decade. The Adriatic Sea response to Bora forcing is most evident in the appearance of several counterrotating gyres, while the sea influences the atmosphere through modification of surface winds and surface heat exchange. Several interesting phenomena occur related to the Bora flow, usually on smaller mesoscales to microscales. These include mountain wave-induced rotors and lee vortexes with horizontal axes characterized by strong updrafts and downdrafts and turbulence that, among other problems, present a danger to air traffic. Also, the gusty Bora nature is shown to be modulated by quasi-periodic pulsations on timescales of several minutes. A more

detailed description of the Bora wind can be found in a review by Grisogono and Belušić´ (2009) and references therein.

A wind similar to Bora in terms of general mechanisms is *Mistral*/Tramontane. Mistral, with Tramontane being a branch of basically the same system, is a north-to-northwesterly wind blowing over southeastern France and the Gulf of Lions. It is also a complex superposition of gap and downslope flows, but with an orographic setup different from that for Bora, it takes on a somewhat different final shape (Jiang et al., 2003; Guénard et al., 2006; Lebeaupin Brossier and Drobinski, 2009). Both Bora and Mistral advect cold air to the affected areas. Another example of orographically enhanced winds is *Levanter* in the Strait of Gibraltar (Dorman et al., 1995; Capon, 2006).

A number of other local winds exist that are similar to the above-mentioned well-known winds (Koletsis et al., 2009) but are either not as persistent or do not influence the local population to an extent sufficient to obtain a name and detailed studies. However, only a couple of the main Mediterranean winds are described here, particularly those of orographic origin. Many other local winds in the region, or even the same winds but with different names, have not been discussed here. A schematic of the main Mediterranean winds is shown in Lionello et al. (2006b, figure 116).

5.6.3 Dust Storms

Dust storms, which occur when strong winds blow dust and sand from a dry surface, are a major hazard in the MR. They are related to the occurrence of strong winds in the areas along the southern Mediterranean Coast, and these are in turn related to synoptic-scale weather systems at the surface and at upper levels (Thorncroft and Flocas, 1997; see also Section 5.3.5). Typical examples are Khamsin depressions, also known as Sharav or desert depressions, that form in the lee of the Atlas Mountains and then track eastward or northeastward and cause dust storms along the Mediterranean coast (El Fandy, 1940; Pedgley, 1972; Yaalon and Ganor, 1979; Alpert and Ziv, 1989). In the western part, the cold air to the west of the upper-level disturbance can be blocked by the Atlas Mountains and then create dust storms in the Tunisian/Algerian Chotts region when surging into the Sahara around the eastern end of the mountain chain (Knippertz et al., 2009). Farther east, the cold air can penetrate unimpeded into the Libyan and Egyptian Deserts and even into the Middle East sometimes, behind a cold front associated with widespread dust-storm activity. The fast increase of pressure to the east of the cyclone can in turn enhance the North African *Harmattan* trade wind over the Sahara and cause dust storms farther south (Knippertz and Fink, 2006; Washington and Todd, 2005). In cases of deep dust layers, plumes can be transported northward ahead of upper-level disturbances and reach the northern Mediterranean countries (Sodemann et al., 2006).

During the warm season, deep moist convection regularly forms over the peaks of the Atlas Mountains in Morocco and Algeria. In situations of favorable wind shear, evaporation of precipitation on the hot and dry southern side creates extended cold air pools that propagate into the northern Sahara in the form of density currents of up to several hundred kilometers in scale (Knippertz et al., 2007; Emmel et al., 2010).

Dust storms are then mostly confined to the leading edge, where strong gusty winds are commonly observed.

5.6.4 Marine Storms

The effects of cyclones passing over Europe and the triggering of lee cyclones consistently induces waves and storm-surge activity over the northern basins of the Mediterranean. Several studies have considered in detail the Gulf of Lions and the northern Adriatic in this respect (Trigo et al., 2002a; Lionello, 2005; Lionello et al., 2010). However, the northern part of the Aegean Sea is affected by the same type of events (Marcos et al., 2009; Krestenitis et al., 2010).

As in the Adriatic area, the Gulf of Lions is widely open to onshore southerly winds and extratropical storms moving along a southern track between the middle Atlantic and the Mediterranean Sea. This can cause storm surges when a cyclone center in the North Atlantic travels south of 55°N. In this situation, strong southerly winds ahead of the cyclone center blow over the Gulf of Lions toward the coast, leading to a regional-scale sea surge (Ullmann and Moron, 2007). Most of sea surges around the Gulf of Lions occur during the two weather patterns called "Greenland Above" and "Blocking," which are both associated with the negative phase of the NAO. The Greenland Above weather pattern shares features with the negative NAO phase because it shows an anomalous anticyclone over Greenland and a deep low pressure centered around 48–50°N over the eastern North Atlantic. The flow allows synoptic perturbations to reach Europe, but on a more southerly track than usual. The Blocking pattern exhibits typical high pressure extending from the eastern Atlantic to Scandinavia and eastern Europe, during which cyclones are shifted toward the extreme northeast North Atlantic or travel over the Mediterranean Sea (Plaut and Simonnet, 2002).

The Gulf of Venice, in the northern Adriatic Sea, is a hot spot in the Mediterranean for marine storminess, mainly in relation to storm surges. The interest in this area is justified not only by the presence of a unique city that is endangered by high storm surges (Canestrelli et al., 2001), such as that which happened in 1966 (De Zolt et al., 2006), but also by its environmental characteristics: the northern Adriatic is where sea-level maxima are largest in the Mediterranean (Marcos et al., 2009) and is directly impacted by the lee cyclones formed in the western Mediterranean. Surges are directly produced by cyclones, but their frequency is linked to large-scale patterns on the seasonal timescale, and favorable conditions are associated with planetary waves.

A large-scale pattern associated with periods with frequent high storm-surge events has been described in Lionello (2005) and Barriopedro et al. (2010). It presents a cyclonic center of action located above western Europe, which favors the penetration of cyclones into the MR (see also Section 5.3). Preconditioning for storm surges has been found to be linked with the low-frequency disturbances of air pressure and wind that are associated with planetary atmospheric waves in the range of 0.1–0.01 cycles per day and account for one third of total sea-level variability. These disturbances can give rise to sea-level changes in the range of 70 cm, thus posing strong preconditions, lasting days, for flooding (Pasarić and Orlic, 2001).

However, individual cyclones are the main factor responsible for peak storm surges. The synoptic patterns leading to storm surges are well known (Robinson et al., 1973). A persistent deep low-pressure system located west of the basin induces a pressure gradient with a large southeastward component along the basin. These synoptic situations have been shown to originate very often from a large low-pressure system above northern Europe (Trigo and Davies, 2002). Channeling effects caused by the long coastal mountain ridges intensify and steer a strong Sirocco wind, which accumulates water at the northern coast and produces high waves because of its long fetch. General characteristics of these cyclones are discussed in the literature (Lionello, 2005; Lionello et al., 2006a, 2010). Intense cyclonic circulation is a basic characteristic for cyclones producing severe marine storms, but it is not sufficient by itself. Cyclones producing high surges tend to originate in the western Mediterranean, with most of the cyclones affecting northern Italy born in the Gulf of Genoa. This is because the tracks of cyclones originating in the western Mediterranean can favor an intense wind along the main axis of the Adriatic Sea, in general producing waves and sea surge simultaneously. However, the paths of cyclones producing severe surges and of those producing very high waves differ, and the latter tend to follow a more southerly path, which is consistent with an action of the wind that is more efficient in the central and southern part of the Adriatic than in the northern part (Lionello et al., 2010).

5.6.5 Ocean-Wave Variability

Most studies of wave variability are based on numerical hindcasts, because, while instrumental wave records are too sparse and satellite time series too short for the identification of climate trends, numerical simulations can be organized to cover the whole Mediterranean basin for multidecadal periods. Although hindcasted model data usually underestimate the actual significant wave height (SWH) as compared with buoy observations, satellite data, and simulations forced by higher-resolution wind fields, they provide a reliable representation of the real space and time variability (Lionello and Sanna, 2005).

Some analyses have concentrated on NAO and have shown that the winter average SWH in the Mediterranean Sea is anticorrelated with the winter NAO Index. During summer, a component of the wave-field interannual variability presents a statistically significant correlation with the Indian monsoon reflecting its influence on the meridional Mediterranean circulation (Lionello and Sanna, 2005). However, the SLP patterns associated with the SWH interannual variability reveal structures different from those of NAO and monsoon circulation, and small subareas can behave differently with respect to the rest of the basin. In fact, when the NAO is in its positive phase, positive anomalies in SWHs and the 95th percentile SWH appear in the area between the Balearic Islands, the Gulf of Lions, and the Catalonia coast (Cañellas et al., 2010).

In general, several midlatitude patterns are linked to the average SWH field in the Mediterranean (Lionello and Galati, 2008), especially in its western part during the cold season: East Atlantic pattern (EA), Scandinavian pattern (SCAND), NAO, East Atlantic/West Russia pattern (EA/WR), and East Pacific/North Pacific pattern (EP/NP). Though the EA pattern exerts the largest influence, it is not sufficient to

characterize the dominant variability. NAO, though relevant, has an effect smaller than that of EA and comparable to other patterns. Similar considerations apply to extreme SWH, which, however, are more influenced by these midlatitude teleconnections in winter and fall than in other seasons (Pino et al., 2010).

5.7 Conclusion

The climate of the MR is characterized by a complex interaction of large-scale atmospheric patterns, the Mediterranean Ocean, and orographic factors. In the previous chapters, we summarized findings from scientific studies that extracted basic statistical relationships and identified underlying physical mechanisms. While there is a good basic understanding of many features of the Mediterranean climate, it was not always possible to provide a straightforward and unequivocal description for all of them. This is partly due to our limited knowledge of past climate, which is a particular problem with respect to the occurrence of extreme events. However, even the relationships of local synoptic events and the large-scale patterns affecting the MR are not always stable in time and space. It can be assumed that one of the reasons is a high sensitivity of the MR climate to remote influences from the midlatitudes and from the lower latitudes. In this context, the role of nonlinear feedback processes (as, for example, the generation and growth of cyclones, depending inter alia on the relationship of the complex orography and the large-scale airflow) is evidently relevant. Numerical modeling of the Mediterranean climate and its features has been an important basis for the scientific results described in previous chapters. This refers not only to the physical understanding of some processes, but even to the availability of long-term time series of climate parameters for which measurements are not available at sufficient density and extension in time and space (e.g., ocean waves). Because this is true for many other aspects of research on the Mediterranean climate, further scientific progress can be expected to be based on a combination of improving numerical models and data analysis.

Acknowledgments

The authors thank Isabel Trigo and Radan Huth for their comments, suggestions, and constructive review of this chapter.

References

Alpert, P., Reisin, T., 1986. An early winter polar air mass penetration to the Eastern Mediterranean. Mon. Weather Rev. 114, 1411–1418.

Alpert, P., Shafir, H., 1989. Meso g-scale distribution of orographic precipitation: numerical study and comparison with precipitation derived from radar measurements. J. Appl. Meteorol. 28, 1105–1117.

Alpert, P., Ziv, B., 1989. The Sharav cyclone: observation and some theoretical considerations. J. Geophys. Res. 94, 18495–18514.

Alpert, P., Neeman, B.U., Shay-El, Y., 1990a. Climatological analysis of Mediterranean cyclones using ECMWF data. Tellus 42A, 65–77.

Alpert, P., Abramsky, R., Neeman, B.U., 1990b. The prevailing summer synoptic system in Israel—subtropical high, not Persian trough. Isr. J. Earth Sci. 39, 93–102.

Alpert, P., Tzidulko, M., Krichak, S., Stein, U., 1996. A multi-stage evolution of an ALPEX cyclone. Tellus 48A, 209–220.

Alpert, P., Ben-Gai, T., Baharad, A., Benjamini, Y., Yekutieli, D., Colacino, M., et al., 2002. The paradoxical increase of Mediterranean extreme daily rainfall in spite of decrease in total values. Geophys. Res. Lett. 29. doi: 10.1029/2001GL013554.

Alpert, P., Osetinsky, I., Ziv, B., Shafir, H., 2004a. Semi-objective classification for daily synoptic systems, application to the eastern Mediterranean climate change. Int. J. Climatol. 24, 1001–1011.

Alpert, P., Osetinsky, I., Ziv, B., Shafir, H., 2004b. A new seasons definition based on classified daily synoptic systems: an example for the eastern Mediterranean. Int. J. Climatol. 24, 1013–1021.

Alpert, P., Baldi, M., Ilani, R., Krichak, S., Price, C., Rodó, X., et al., 2006. Relations between climate variability in the Mediterranean region and the Tropics: ENSO, South Asian and African monsoons, Hurricanes and Saharan Dust In: Lionello, P. Malanotte-Rizzoli., P. Boscolo, R. (Eds.), The Mediterranean Climate: An Overview of the Main Characteristics and Issues. Elsevier, Amsterdam, pp. 149–177.

Ashbel, D., 1938. Great floods in Sinai Peninsula, Palestine, Syria and the Syrian desert, and the influence of the Red Sea on their formation. Q. J. R. Meteorol. Soc. 64, 635–639.

Baldi, M., Meneguzzo, F., Dalu, G.A., Maracchi, G., Pasqui, M., Capecchi, V., et al., 2006. Guinea Gulf SST and Mediterranean summer climate: analysis of the interannual variability. <http://www.pdfli.com/57984/climate-analysis/>.

Barnston, G., Livezey, R.E., 1987. Classification, seasonality and low-frequency atmospheric circulation patterns. Mon. Weather Rev. 115, 1083–1126.

Barredo, J.I., 2009. Normalised flood losses in Europe. Nat. Hazards Earth Syst. Sci. 9, 97–104.

Barriopedro, D., Garcia-Herrera, R., Lionello, P., Pino, C., 2010. A discussion of the links between solar variability and high storm surge events in Venice. J. Geophys. Res. 115, D13101. doi: 10.1029/2009JD013114.

Barry, R.G., Chorley, R.J., 1998. The African Monsoon. Atmosphere Weather and Climate, seventh ed. Routledge, 11 New Fetter Lane, LondonEC4P 4EE, UK, p. 409.

Bartholy, J., Pongrácz, R., Pattantyús-Ábrahám, M., 2009. Analyzing the genesis, intensity, and tracks of western Mediterranean cyclones. Theor. Appl. Climatol. 96, 133–144.

Becker, N., 2010. Wind-Analyse hoch aufgelöster Simulationen für den Mittelmeerraum. Master's Thesis. Institute for Meteorology, Freie Universität Berlin, Berlin.

Belušić, D., Guttler, I., 2010. Can mesoscale models reproduce meandering motions? Q. J. R. Meteorol. Soc. 136 (648), 553–565.

Beniston, M., 2007. Linking extreme climate events and economic impacts: examples from the Swiss Alps. Energy Policy 35, 5384–5392.

Bergeron, T., 1954. The problem of tropical hurricanes. Q. J. R. Meteorol. Soc. 80, 131–164. doi: 10.1002/qj.49708034402.

van den Besselaar, E.J.M., Klein Tank, A.M.G., van der Schrier, G., 2010. Influence of circulation types on temperature extremes in Europe. Theor. Appl. Climatol. 99, 431–439.

Bitan, A., Saaroni, H., 1992. The horizontal and vertical extension of the Persian Gulf trough. Int. J. Climatol. 12, 733–747.

Brönnimann, S., Xoplaki, E., Casty, C., Pauling, A., Luterbacher, 2007. ENSO influence on Europe during the last centuries. J. Clim. Dyn. 28 (2–3), 181–197.

Brunet, M., Jones, P.D., Sigró, J., Saladié, O., Aguilar, E., Moberg, A., et al., 2007a. Temporal and spatial temperature variability and change over Spain during 1850–2005 J. Geophys. Res. 112, doi: 10.1029/2006JD008249.

Brunet, M., Sigró, J., Jones, P.D., Saladié, O., Aguilar, E., Moberg, A., et al., 2007b. Long-term changes in extreme temperatures and precipitation in Spain. Contrib. Sci. 3, 331–342.

Brunetti, M., Lentini, G., Maugeri, M., Nanni, T., Auer, I., Böhm, R., et al., 2009. Climate variability and change in the Greater Alpine Region over the last two centuries based on multi-variable analysis. Int. J. Climatol. 29 (15), 2197–2225.

Burlando, M., 2009. The synoptic-scale surface wind climate regimes of the Mediterranean Sea according to the cluster analysis of ERA-40 wind fields. Theor. Appl. Climatol. 96, 69–83.

Buzzi, A., Tibaldi, S., 1978. Cyclogenesis in the lee of the Alps: a case study. Q. J. R. Meteorol. Soc. 104, 271–287.

Buzzi, A., Richard, E., Romero, R., 2005. Summary Report on MEDEX Studies and Scientific Results on Mediterranean Cyclones Causing High Impact Weather. MEDEX Project. <http://medex.aemet.uib.es/index.html>.

Campins, J., Genoves, A., Jansa, A., Guijarro, J.A., Ramis, C., 2000. A catalogue and a classification of surface cyclones for the western Mediterranean. Int. J. Climatol. 20, 969–984.

Campins, J., Genovés, A., Picornell, M.A., Jansà, A., 2011. Climatology of Mediterranean cyclones using the ERA-40 dataset. Int. J. Climatol. doi: 10.1002/joc.2183.

Cañellas, B., Orfila, A., Méndez, F., Álvarez, A., Tintoré, J., 2010. Influence of the NAO on the northwestern Mediterranean wave climate. Sci. Mar. 74, 55–64.

Canestrelli, P., Mandich, M., Pirazzoli, P.A., Tomasin, A., 2001. Wind, Depression and Seiches: Tidal Perturbations in Venice (1951–2000). Centro Previsioni e Segnalazioni Maree, Venezia, p. 107.

Capon, R.A., 2006. High resolution studies of the Gibraltar Levanter validated using sun-glint anemometry. Meteorol. Appl. 13, 257–265.

Carril, A.F., Gualdi, S., Cherchi, A., Navarra, A., 2008. Heatwaves in Europe: areas of homogeneous variability and links with the regional to large-scale atmospheric and SSTs anomalies. Clim. Dyn. 30 (1), 77–98.

Cassou, C., Terray, L., Phillips, A.S., 2005. Tropical Atlantic influence on European heat waves. J. Clim. 18 (15), 2805–2811.

Casty, C., Handorf, D., Sempf, M., 2005b. Combined winter climate regimes over the North Atlantic/European sector 1766–2000. Geophys. Res. Lett. 32 (13), L13801.

Casty, C., Handorf, D., Raible, C.C., González-Rouco, J.F., Weisheimer, A., Xoplaki, E., et al., 2005a. Recurrent climate winter regimes in reconstructed and modelled 500 hPa geopotential height fields over the North Atlantic/European sector 1659–1990. Clim. Dyn. 24 (7–8), 809–822.

Cattiaux, J., Vautard, R., Yiou, P., 2011. North-Atlantic SST amplified recent wintertime European land temperature extremes and trends. Clim. Dyn. 36, 2113–2128. doi: 10.1007/s00382-010-0869-0.

Christiansen, B., 2009. Is the atmosphere interesting? A projection pursuit study of the circulation in the Northern Hemisphere winter. J. Clim. 22 (5), 1239–1254.

Coles, S., 2001. An Introduction to Statistical Modeling of Extreme Values. Springer, London, UK.

Conte, M., 1986. The meteorological "bomb" in the Mediterranean: a synoptic climatology. Rivista di Meteorologia Aeronautica XLVI 314, 121–130.

Conte, M., Piervitali, E., Colacino, M., 1997. The meteorological bomb in the Mediterranean. INM/WMO International Symposium on Cyclones and Hazardous Weather in the Mediterranean MMA/UIB, pp. 283–287.

Corti, S., Molteni, F., Palmer, T.N., 1999. Signature of recent climate change in frequencies of natural atmospheric circulation regimes. Nature 398 (6730), 799–802.

Croci-Maspoli, M., Schwierz, C., Davies, H.C., 2007. A multifaceted climatology of atmospheric blocking and its recent linear trend. J. Clim. 20 (4), 633–649.

Dayan, U., Rodnizki, J., 1999. The temporal behavior of the atmospheric boundary layer in Israel. J. Appl. Meteorol. 38, 830–836.

Dayan, U., Shenhav, R., Graber, M., 1988. The spatial and temporal behavior of the mixed layer in Israel. J. Appl. Meteorol. 27, 1382–1394.

Dayan, U., Ziv, B., Margalit, A., Morin, E., Sharon, D., 2001. A severe autumn storm over the middle-east: synoptic and mesoscale convection analysis. Theor. Appl. Climatol. 69 (1–2), 103–122.

Dayan, U., Lifshitz-Goldreich, B., Pick, K., 2002. Spatial and structural variation of the atmospheric boundary layer during summer in Israel—profiler and rawinsonde measurements. J. Appl. Meteorol. 41, 447–457.

De Zolt, S., Lionello, P., Malguzzi, P., Nuhu, A., Tomasin, A., 2006. The disastrous storm of 4 November 1966 on Italy. Nat. Hazards Earth Syst. Sci. 6, 861–879.

Della-Marta, P.M., Haylock, M.R., Luterbacher, J., Wanner, H., 2007a. Doubled length of western European summer heat waves since 1880. J. Geophys. Res. 112, D15.

Della-Marta, P.M., Luterbacher, J., von Weissenfluh, H., Xoplaki, E., Brunet, M., Wanner, H., 2007b. Summer heat waves over western Europe 1880–2003, their relationship to large-scale forcings and predictability. Clim. Dyn. 29 (2–3), 251–275.

Dorman, C.E., Beardsley, R.C., Limeburner, R., 1995. Winds in the Strait of Gibraltar. Q. J. R. Meteorol. Soc. 121, 1903–1921.

Dünkeloh, A., Jacobeit, J., 2003. Circulation dynamics of Mediterranean precipitation variability. Int. J. Climatol. 23, 1843–1866.

Duffourg, F., Ducrocq, V., 2011. Origin of the moisture feeding the heavy precipitating systems over Southeastern France. Nat. Hazards Earth Syst. Sci. 4, 1163–1178.

Egger, J., 1995. Interaction of cold-air blocking and upper-level potential vorticity anomalies during lee cyclogenesis. Tellus A 47, 597–604.

Egger, J., Alpert, P., Tafferner, A., Ziv, B., 1995. Numerical experiments on the genesis of Sharav cyclones: idealized simulation. Tellus 47A, 162–174.

El Fandy, M.G., 1940. The formation of depressions of the Khamsin type. Q. J. R. Meteorol. Soc. 66, 323–336.

El Fandy, M.G., 1948. The effect of the Sudan monsoon low on the development of thundery conditions in Egypt, Palestine and Syria. Q. J. R. Meteorol. Soc. 74, 31–38.

El Kenawy, A.M., López-Moreno, J.L., Vicente-Serrano, S.M., Mekld, M.S., 2009. Temperature trends in Libya over the second half of the 20th century. Theor. Appl. Climatol. 98 (1–2), 1–8.

Emmel, C., Knippertz, P., Schulz, O., 2010. Climatology of convective density currents in the southern foothills of the Atlas Mountains. J. Geophys. Res. doi: 10.1029/2009JD12863.

Feudale, L., Shukla, J., 2007. Role of Mediterranean SST in enhancing the European heat wave of summer 2003. Geophys. Res. Lett. 34 (3), L03811.

Fischer, E.M., Seneviratne, S.I., Lüthi, D., Schär, C., 2007. Contribution of land–atmosphere coupling to recent European summer heat waves. Geophys. Res. Lett. 34, L06707. doi: 10.1029/2006GL029068.

Flocas, H.A., 2000. Diagnostics of cyclogenesis over the Aegean Sea using potential vorticity inversion. Meteorol. Atmos. Phys. 73, 25–33.

Flocas, A.A., Karacostas, T.S., 1996. Cyclogenesis over the Aegean Sea: identifications and synoptic categories. Meteorol. Appl. 3, 53–61.

Flocas, H.A., Simmonds, I., Kouroutzoglou, J., Keay, K., Hatzaki, M., Bricolas, V., et al., 2010. On cyclonic tracks over the eastern Mediterranean. J. Clim. 23 (19), 5243–5257.

Goldreich, Y., 2003. The Climate of Israel: Observation, Research and Application. Springer/ Kluwer Academic/Plenum Publishers, Israel/The Netherlands, p. 298.

Goubanova, K., Li, L., Yiou, P., Codron, F., 2010. Relation between large-scale circulation and European winter temperature: does it hold under warmer climate? J. Clim. 23 (13), 3752–3760.

Grisogono, B., Belušić, D., 2009. A review of recent advances in understanding the meso- and microscale properties of the severe Bora wind. Tellus 61A, 1–16.

Guénard, V., Drobinski, P., Caccia, J.L., Tedeschi, G., Currier, P., 2006. Dynamics of the MAP IOP 15 severe Mistral event: observations and high-resolution numerical simulations. Q. J. R. Meteorol. Soc. 132, 757–777.

Hannachi, A., 2010. On the origin of planetary-scale extratropical winter circulation regimes. J. Atmos. Sci. 67 (5), 1382–1401.

Hatzaki, M., Flocas, H.A., Asimakopoulos, D.N., Maheras, P., 2007. The eastern Mediterranean teleconnection pattern: identification and definition. Int. J. Climatol. 27, 727–737.

Hatzaki, M., Flocas, H.A., Giannakopoulos, C.H., Maheras, P., 2009. The impact of the eastern Mediterranean teleconnection pattern at the Mediterranean climate. J. Clim. 22, 977–992.

Harats, N., Ziv, B., Yair, Y., Kotroni, V., Dayan, U., 2010. Dynamic and thermodynamic predictors for lightning and flash floods in the Mediterranean. Adv. Geosci. 23, 57–64.

HMSO, 1962. Weather in the Mediterranean I: General Meteorology, second ed. Her Majesty's Stationery Office, London, p. 362.

Homar, V., Jansa, A., Campins, J., Genoves, A., Ramis, C., 2007. Towards a systematic climatology of sensitivities of Mediterranean high impact weather: a contribution based on intense cyclones. Nat. Hazards Earth Syst. Sci. 7, 445–454.

Hurrell, J.W., van Loon, H., 1997. Decadal variations in climate associated with the north Atlantic oscillation. Clim. Change 36, 301–326.

Huth, R., Benestad, R., Lionello, P., 2009. Editorial for special issue of Theor. Appl. Climatol. on "Synoptic Climatology". Theor. Appl. Climatol. 96, 1.2. doi: 10.1007/s00704-008-0077-6.

Jacobeit, J., Dünkeloh, A., Hertig, E., 2007. Mediterranean rainfall changes and their causes. In: Lozán, J., Graßl, H., Hupfer, P., Menzel, L., Schönwiese, C.-D. (Eds.), Global Change: Enough Water for All? Hamburg, 2007, pp. 195–199.

Jaeger, E.B., Anders, I., Lüthi, D., Rockel, B., Schär, C., Seneviratne, S.I., 2008. Analysis of ERA40-driven CLM simulations for Europe. Meteorol. Z. 17, 349–367.

Jansa, A., Genoves, A., Picornell, M.A., Campins, J., Riosalido, R., Carretero, O., 2001. Western Mediterranean cyclones and heavy rain. Part 2: statistical approach. Meteorol. Appl. 8, 43–56.

Jiang, Q., Smith, R.B., Doyle, J., 2003. The nature of the mistral: observations and modelling of two MAP events. Q. J. R. Meteorol. Soc. 129, 857–875.

Kafle, H.K., Bruins, H.J., 2009. Climatic trends in Israel 1970–2002: warmer and increasing aridity inland. Clim. Change 96 (1–2), 63–77.

Kahana, R., Ziv, B., Enzel, Y., Dayan, U., 2002. Synoptic climatology of major floods in the Negev desert, Israel. Int. J. Climatol. 22, 867–882.

Kalnay, E., Kanamitsu, M., Kistler, R., Collins, W., Deaven, D., Gandin, L., et al., 1996. The NCEP/NCAR 40-year reanalysis project. Bull. Am. Meteorol. Soc. 77, 437–471.

Karacostas, T.S., Flocas, A.A., 1983. The development of the "bomb" over the Mediterranean area. La Meteorologie. Actes de la Conference "eau verte" 34, 351–358.

Kioutsioukis, I., Melas, D., Zerefos, C., 2010. Statistical assessment of changes in climate extremes over Greece. Int. J. Climatol. 30, 1723–1737.

Kistler, R., et al., 2001. The NCEP–NCAR 50-year reanalysis: monthly means CD-ROM and documentation. Bull. Am. Meteorol. Soc. 82, 247–267.

Klaić, Z.B., Pasarić, Z., Tudor, M., 2009. On the interplay between sea–land breezes and Etesian winds over the Adriatic. J. Mar. Syst. 78, S101–S118.

Klein Tank, A.M.G., Können, G.P., 2003. Trends in indices of daily temperature and precipitation extremes in Europe, 1946–99. J. Clim. 16 (22), 3665–3680.

Klein Tank, A.M.G., Zwiers, F.W., 2009. Guidelines on: analysis of extremes in a changing climate in support of informed decisions for adaptation, WMO-TD 1500.

Knippertz, P., Fink, A.H., 2006. Synoptic and dynamic aspects of an extreme springtime Saharan dust outbreak. Q. J. R. Meteorol. Soc. 132, 1153–1177.

Knippertz, P., Ulbrich, U., Marques, F., Corte-Real, J., 2003. Decadal changes in the link El Niño, NAO and European/North African rainfall. Int. J. Climatol. 23, 1293–1311.

Knippertz, P., Deutscher, C., Kandler, K., Müller, T., Schulz, O., Schütz, L., 2007. Dust mobilization due to density currents in the Atlas region: observations from the SAMUM 2006 field campaign. J. Geophys. Res. 112, D21109. doi: 10.1029/2007JD008774.

Knippertz, P., Ansmann, A., Althausen, D., Müller, D., Tesche, M., Bierwirth, E., et al., 2009. Dust mobilization and transport in the northern Sahara during SAMUM 2006—a meteorological overview. Tellus B 61 (1), 12–31.

Koch, J., Dayan, U., 1992. A synoptic analysis of the meteorological conditions affecting dispersion of pollutants emitted from tall stacks in the coastal plain of Israel. Atmos. Environ. 26A (14), 2537–2543.

Koletsis, I., Lagouvardos, K., Kotroni, V., Bartzokas, A., 2009. Numerical study of a downslope windstorm in Northwestern Greece. Atmos. Res. 94, 178–193.

Kostopoulou, E., Jones, P.D., 2005. Assessment of climate extremes in the Eastern Mediterranean. Meteorol. Atmos. Phys. 89, 69–85.

Kotroni, V., Lagouvardos, K., Lalas, D., 2001. The effect of the island of Crete on the Etesian winds over the Aegean Sea. Q. J. R. Meteorol. Soc. 127, 1917–1937.

Kouroutzoglou, J., Flocas, H.A., Keay, K., Simmonds, I., Hatzaki, M., 2011. Climatological aspects of explosive cyclones in the Mediterranean. Int. J. Climatol. 31, 1785–1802. doi: 10.1002/joc.2203.

Krestenitis, Y.N., Androulidakis, Y.S., Kontos, Y.N., Georgakopoulos, G., 2010. Coastal inundation in the north-eastern Mediterranean coastal zone due to storm surge events. J. Coastal Conserv. 14, 1–16. doi: 10.1007/s11852-010-0090-7.

Krichak, S.O., Alpert, P., 1998. Role of large scale moist dynamics in November 1–5, 1994, hazardous Mediterranean weather. J. Geophys. Res. 103, 19453–19468.

Krichak, S.O., Alpert, P., Dayan, M., 2004. Role of atmospheric processes associated with hurricane Olga in December 2001 floods in Israel. J. Hydrometeorol. 5, 1259–1270.

Krichak, S.O., Kishcha, P., Alpert, P., 2002. Decadal trends of main Eurasian oscillations and the Mediterranean precipitation. Theor. Appl. Climatol. 72, 209–220.

Kuglitsch, F.G., Toreti, A., Xoplaki, E., Della-Marta, P.M., Zerefos, C.S., Türke , M., et al., 2010. Heat wave changes in the eastern Mediterranean since 1960. Geophys. Res. Lett. 37, L04802.

Lagouvardos, K., Kotroni, V., Defer, E., 2007. The 21–22 January 2004 explosive cyclogenesis over the Aegean Sea: observations and model analysis. Q. J. R. Meteorol. Soc. 133, 1519–1531. doi: 10.1002/qj.121.

Lebeaupin Brossier, C., Drobinski, P., 2009. Numerical high-resolution air–sea coupling over the Gulf of Lions during two tramontane/mistral events. J. Geophys. Res. 114, D10110.

Leckebusch, G.C., Renggli, D., Ulbrich, U., 2008. Development and application of an objective storm severity measure for the Northeast Atlantic region. Meteorol. Z. 17 (5), 575–587. doi: 10.1127/0941-2948/2008/0323.

Liberato, M.L.R., Pinto, J.G., Trigo, I.F., Trigo, R.M., 2011. Klaus—an exceptional winter storm over northern Iberia and southern France. Weather 66, 330–334. doi: 10.1002/wea.755.

Lionello, P., 2005. Extreme surges in the Gulf of Venice. Present and future climate. In: Fletcher, C., Spencer, T. (Eds.), Venice and its Lagoon. State of Knowledge. Cambridge University Press, Cambridge, UK, pp. 59–65.

Lionello, P., Galati, M.B., 2008. Links of the significant wave height distribution in the Mediterranean Sea with the North Hemisphere teleconnection patterns. Adv. Geosci. 17, 13–18.

Lionello, P., Sanna, A., 2005. Mediterranean wave climate variability and its links with NAO and Indian Monsoon. Clim. Dyn. 25, 611–623.

Lionello, P., Dalan, F., Elvini, E., 2002. Cyclones in the Mediterranean region: the present and the doubled CO_2 climate scenarios. Clim. Res. 22, 147–159.

Lionello, P., Bhend, J., Buzzi, A., Della-Marta, P.M., Krichak, S., Jansà, A., et al., 2006a. Cyclones in the Mediterranean region: climatology and effects on the environment. In: Lionello, P., Malanotte-Rizzoli, P., Boscolo, R. (Eds.), Mediterranean Climate Variability. Elsevier, Amsterdam, The Netherlands, pp. 325–372. (Developments in Earth and Environmental Sciences 4 (C)).

Lionello, P., Malanbotte-Rizzoli, P., Boscolo, R. (Eds.), 2006b. Mediterranean Climate Variability, Developments in Earth and Environmental Sciences 4. Elsevier, Radarweg 29, Amsterdam, The Netherlands

Lionello, P., Cavaleri, L., Nissen, K., Pino, C., Raicich, F., Ulbrich, U., 2010. Marine storminess in the Northern Adriatic: characteristics and trends. Phys. Chem. Earth doi: 10.1016/j.pce.2010.10.002.

Liu, X., Yanai, M., 2001. Relationship between the Indian monsoon rainfall and the tropospheric temperature over the Eurasian continent. Q. J. R. Meteorol. Soc. 127, 909–938.

Lopez, J.M., 2005. A Mediterranean derecho: Catalonia (Spain), 17th August 2003. Atmos. Res. 83 (2007), 272–283.

López-Moreno, J.I., Vicente-Serrano, S.M., Angulo-Martínez, M., Beguería, S., Kenawy, A., 2010. Trends in daily precipitation on the northeastern Iberian Peninsula. Int. J. Climatol. 30, 1026–1041.

Luterbacher, J., Liniger, M.A., Menzel, A., Estrella, N., Della-Marta, P.M., Pfister, C., et al., 2007. Exceptional European warmth of autumn 2006 and winter 2007: historical context, the underlying dynamics, and its phenological impacts. Geophys. Res. Lett 34 (12), L12704.

Maheras, P., 1980. Le problème des Etésiens. Méditerranée 40, 57–66.

Maheras, P., Xoplaki, E., Davies, T., Martin-Vide, J., Bariendos, M., Alcoforado, M.J., 1999. Warm and cold monthly anomalies across the Mediterranean basin and their relationship with circulation; 1860–1990. Int. J. Climatol. 19, 1697–1715.

Maheras, P., Flocas, H., Patrikas, I., Anagnostopoulou, C., 2001. A 40 year objective climatology of surface cyclones in the Mediterranean region: spatial and temporal distribution. Int. J. Climatol. 21, 109–130.

Maheras, P., Flocas, H.A., Anagnostopoulou, C., Patrikas, I., 2002. On the vertical structure of composite surface cyclones in the Mediterranean region. Theor. Appl. Climatol. 71, 199–217.

Marcos, M., Tsimplis, M.N., Shaw, A.G.P., 2009. Sea level extremes in Southern Europe. J. Geophys. Res. 114, C01007. doi: 10.1029/2008JC004912.

Mariotti, A., Zeng, N., Lau, K.M., 2002. Euro-Mediterranean rainfall and ENSO—a seasonally varying relationship. Geophys. Res. Lett. 29, 1621, 4 PP. doi: 10.1029/2001GL014248.

Mariotti, A., Ballabrera-Poy, J., Zeng, N., 2005. Tropical influence on Euro-Asian autumn rainfall variability. Clim. Dyn. 24, 511–521.

Martín, M.L., Luna, M.Y., Morata, A., Valero, F., 2004. North Atlantic teleconnection patterns of low-frequency variability and their links with springtime precipitation in the western Mediterranean. Int. J. Climatol. 24, 213–230.

McGinley, J., Zupanski, M., 1990. Numerical analysis of jets, fronts, and mountains on Alpine lee cyclogenesis. Meteorol. Atmos. Phys. 43, 7–20.

McGuinley, J., 1982. A diagnosis of Alpine lee cyclogenesis. Mon. Weather Rev. 110, 1271–1287.

Metaxas, D.A., 1977. The interannual variability of the Etesian frequency as a response of atmospheric circulation anomalies. Bull. Hellenic Meteorol. Soc. 2 (5), 30–40.

Michelangeli, P.A., Vautard, R., Legras, B., 1995. Weather regimes—recurrence and quasi stationarity. J. Atmos. Sci. 52 (8), 1237–1256.

Miranda, P.M.A., Tomé, A.R., 2009. Spatial structure of the evolution of surface temperature (1951–2004). Clim. Change 93 (1–2), 269–284.

Moberg, A., Jones, P.D., Lister, D., Walther, A., Brunet, M., Jacobeit, J., et al., 2006. Indices for daily temperature and precipitation extremes in Europe analyzed for the period 1901–2000. J. Geophys. Res. 111 (D22), D22106.

Munich, Re, 2010. Analyses, assessments, positions. Topics GEO. Munich Re, München.

Musculus, M., Jacob, D., 2005. Tracking cyclones in regional model data: the future of Mediterranean storms. Adv. Geosci. 2, 13–19.

Nissen, K.M., Leckebusch, G.C., Pinto, J.G., Renggli, D., Ulbrich, S., Ulbrich, U., 2010. Cyclones causing wind storms in the Mediterranean: characteristics, trends and links to large-scale patterns. Nat. Hazards Earth Syst. Sci. 10, 1379–1391.

Nogaj, M., Yiou, P., Parey, S., Malek, F., Naveau, P., 2006. Amplitude and frequency of temperature extremes over the North Atlantic region. Geophys. Res. Lett. 33, L10801. doi: 10.1029/2005GL024251.

Norrant, C., Douguédroit, A., 2006. Monthly and daily precipitation trends in the Mediterranean (1950–2000). Theor. Appl. Climatol. 83, 89–106.

van Oldenborgh, G.J., Burgers, G., Tank, A.K., 2000. On the El Niño teleconnection to spring precipitation in Europe. Int. J. Climatol. 20, 565–574.

Osborn, T.J., 2004. Simulating the winter North Atlantic Oscillation: the roles of internal variability and greenhouse gas forcing. Clim. Dyn. 22 (6–7), 605–623.

Pandži , K., Likso, T., 2005. Eastern Adriatic typical wind field patterns and large-scale atmospheric conditions. Int. J. Climatol. 25, 81–98.

Parthasarathy, B., Munot, A.A., Korthawale, D., 1995a. All India monthly and seasonal rainfall series: 1871–1993. Theor. Appl. Climatol. 49, 217–224.

Parthasarathy, B., Munot, A.A., Korthawale, D., 1995b. Monthly and seasonal rainfall series for all-India homogeneous regions and meteorological subdivisions: 1871–1993. Research Report No. RR-065, Indian Institute of Tropical Meteorology, Pune, p. 113.

Pasarić, M., Orlic, M., 2001. Long-term meteorological preconditioning of the North Adriatic coastal floods. Cont. Shelf. Res. 21, 263–278.

Pasarić, Z., Belušić, D., Klaić, Z.B., 2007. Orographic influences on the Adriatic Sirocco wind. Ann. Geophys. 25, 1263–1267.

Pasarić, Z., Belušić, D., Chiggiato, J., 2009. Orographic effects on meteorological fields over the Adriatic from different models. J. Mar. Syst. 78, S90–S100.

Pavan, V., Tibaldi, S., Brankovic, C., 2000. Seasonal prediction of blocking frequency: results from winter ensemble experiments. Q. J. R. Meteorol. Soc. 126 (567), 2125–2142. (Eastern Mediterranean region—a methodological approach. Isr. J. Earth Sci. 52, 47–63).

Pedgley, D., 1972. Desert depression over north-east Africa. Meteorol. Mag. 101, 228–243.

Pettersen, S., 1956. Weather Analysis and Forecasting, vol. I. McGraw-Hill, New York, NY, p. 428.

Philipp, A., Della-Marta, P.M., Jacobeit, J., Fereday, D.R., Jones, P.D., Moberg, A., et al., 2007. Long-term variability of daily North Atlantic-European pressure patterns since 1850 classified by simulated annealing clustering. J. Clim. 20, 4065–4095. doi: 10.1175/JCLI4175.1.

Picornell, M.A., Jansà, A., Genovés, A., Campins, J., 2001. Automated database of mesocyclones from the Hirlam (INM)-0.5° analyses in the Western Mediterranean. Int. J. Climatol. 21, 335–354.

Pino, C., Lionello, P., Galati, M.B., 2010. Characteristics and present trends of wave extremes in the Mediterranean Sea. Geophys. Res. Abs. 12 , EGU2010-5984-1.

Pinto, J.G., Spangehl, T., Ulbrich, U., Speth, P., 2005. Sensitivities of a cyclone detection and tracking algorithm: individual tracks and climatology. Meteorol. Z. 14, 823–838.

Pinto, J.G., Reyers, M., Ulbrich, U., 2011. The variable link between PNA and NAO in observations and in multi-century CGCM simulations. Clim. Dyn. 36, 337–354. doi: 10.1007/s00382-010-0770-x.

Plaut, G., Simonnet, E., 2002. Large-scale circulation classification, weather regimes and local climate over France, the Alps and Western Europe. Clim. Res. 17, 303–324.

Pozo-Vázquez, D., Esteban-Parra, M.J., Rodrigo, F.S., Castro-Díez, Y., 2001. A study of NAO variability and its possible non-linear influences on European surface temperature. Clim. Dyn. 17, 701–715. doi: 10.1007/s003820000137.

Pozo-Vazquéz, D., Gámiz-Fortis, S.R., Tovar-Pescador, J., Esteban-Parra, M.J., Castro-Díez, Y., 2005. El Niño-Southern Oscillation events and associated European winter precipitation anomalies. Int. J. Climatol. 25, 17–31.

Prezerakos, N.G., Michaelides, S.C., 1989. A composite diagnosis in sigma coordinates of the atmospheric energy balance during intense cyclonic activity. Q. J. R. Meteorol. Soc. 115, 463–486. doi: 10.1002/qj.49711548703.

Price, C., 1998. A possible link between El Niño and precipitation in Israel. Geophys. Res. Lett. 25, 3963–3966.

Prieto, L., García-Herrera, R., Díaz, J., Hernández, E., del Teso, T., 2004. Minimum extreme temperatures over Peninsular Spain. Global Planet. Change 44, 59–71.

Radinovic, D., 1986. On the development of orographic cyclones. Q. J. R. Meteorol. Soc. 112 (474), 927–951.

Radinovic, D., 1987. Mediterranean Cyclones and their Influence on the Weather and Climate. WMO, PSMP Report Ser. No. 24, p. 131, Geneva, Switzerland.

Raible, C.C., Blender, R., 2004. Northern Hemisphere mid-latitude cyclone variability in GCM simulations with different ocean representations. Clim. Dyn. 22, 239–248. doi: 10.1007/s00382-003-0380-y.

Raible, C., Luksch, U., Fraedrich, K., 2004. Precipitation and Northern hemisphere regimes. Atmos. Sci. Lett. 5, 43–55.

Raible, C.C., Della-Marta, P., Schwierz, C., Wernli, H., Blender, R., 2008. Northern hemisphere extratropical cyclones: a comparison of detection and tracking methods and different reanalyses. Mon. Weather Rev. 136, 880–897.

Reale, O., Atlas, R., 2001. Tropical cyclone-like vortices in the extratropics: observational evidence and synoptic analysis. Weather Forecasting 16, 7–34.

Reiter, E.R., 1975. Handbook for Forecaster in the Mediterranean, Tech. Paper No, 5-75, Naval Postgraduate School, Monterey, CA, p. 334.

Robinson, A.R., Tomasin, A., Artegiani, A., 1973. Flooding of Venice, phenomenology and prediction of the Adriatic storm surge. Q. J. R. Meteorol. Soc. 99 (422), 688–692.

Rodó, X., 2001. Reversal of three global atmospheric fields linking changes in SST anomalies in the Pacific, Atlantic and Indian Oceans at tropical latitudes and midlatitudes. Clim. Dyn. 18, 203–217.

Rodó, X., Baert, E., Comin, F.A., 1997. Variations in seasonal rainfall in Southern Europe during the present century: relationships with the North Atlantic Oscillation and the El Niño-Southern Oscillation. Clim. Dyn. 13, 275–284.

Rodrigo, F.S., 2010. Changes in the probability of extreme daily precipitation observed from 1951 to 2002 in the Iberian Peninsula. Int. J. Climatol. 30, 1512–1525.

Rodrigo, F.S., Trigo, R.M., 2007. Trends in daily rainfall in the Iberian Peninsula from 1951 to 2002. Int. J. Climatol. 27, 513–529.

Rodríguez-Puebla, C., Encinas, A.H., García-Casado, L.A., Nieto, S., 2010. Trends in warm days and cold nights over the Iberian Peninsula: relationships to large-scale variables. Clim. Change 100 (3–4), 667–684.

Rodwell, M.J., Hoskins, B., 1996. Monsoons and the dynamics of deserts. Q. J. R. Meteorol. Soc. 122, 1385–1404.

Romem, M., Ziv, B., Saaroni, H., 2007. Scenarios in the development of Mediterranean cyclones. Adv. Geosci. 12, 59–65.

Saaroni, H., Ziv, B., 2000. Summer rain episodes in a Mediterranean climate, the case of Israel: climatological–dynamical analysis. Int. J. Climatol. 20, 191–209.

Saaroni, H., Ziv, B., Bitan, A., Alpert, P., 1998. Easterly wind storms over Israel. Theor. Appl. Climatol. 59, 61–77.

Saaroni, H., Halfon, N., Ziv, B., Alpert, P., Kutiel, H., 2010. Links between the rainfall regime in Israel and location and intensity of Cyprus Lows. Int. J. Climatol. 30, 1014–1025.

Sáenz, J., Rodríguez-Puebla, C., Fernández, J., Zubillaga, J., 2001. Interpretation of interannual winter temperature variations over southwestern Europe. J. Geophys. Res. 106, 20641–20652.

Sanders, Gyakum, 1980. Mon. Weather Rev. 108, 1589–1606.

Scaife, A.A., Folland, C.K., Alexander, L.V., Moberg, A., Knight, J.R., 2008. European climate extremes and the North Atlantic Oscillation. J. Clim. 21 (1), 72–83.

Scherrer, S.C., Croci-Maspoli, M., Schwierz, C., Appenzeller, C., 2006. Two-dimensional indices of atmospheric blocking and their statistical relationship with winter climate patterns in the Euro-Atlantic region. Int. J. Climatol. 26 (2), 233–249.

Seneviratne, S.I., Lüthi, D., Litschi, M., Schär, C., 2006. Land–atmosphere coupling and climate change in Europe. Nature 443 (7108), 205–209.

Seubert, S., 2010. Telekonnektionen des Niederschlags im Mittelmeerraum zur Zirkulation in den Tropen. Ph.D. Thesis. University of Augsburg (Germany). <http://opus.bibliothek.uni-augsburg.de/volltexte/2010/1646/>.

Shay-El, Y., Alpert, P., 1991. A diagnostic study of winter diabatic heating in the Mediterranean in relation to cyclones. Q. J. R. Meteorol. Soc. 117, 715–747.

Simolo, C., Brunetti, M., Maugeri, M., Nanni, T., Speranza, A., 2010. Understanding climate change-induced variations in daily temperature distributions over Italy. J. Geophys. Res. 115, D22110.

Sodemann, H., Palmer, A.S., Schwierz, C., Schwikowski, M., Wernli, H., 2006. The transport history of two Saharan dust events archived in an Alpine ice core. Atmos. Chem. Phys. 6, 667–688.

Speranza, A., 1975. The formation of baric depression near the Alps. Ann. Geofis. 28 (2–3), 177–217.

Stein, U., Alpert, P., 1993. Factor separation in numerical simulations. J. Atmos. Sci. 50, 2107–2115.

Stephenson, D.B., Hannachi, A., O'Neill, A., 2004. On the existence of multiple climate regimes. Q. J. R. Meteorol. Soc. 130 (597), 583–605.

Tafferner, A., Egger, J., 1990. Test of theories of lee cyclogenesis: ALPEX cases. J. Atmos. Sci. 47 (20), 2417–2428.

Tantawy, A.H.I., 1969. On the cyclogenesis and structure of spring Sahara depressions in the subtropical Africa. Meteorol. Res. Bull. 69, 68–107. United Arab Republic, Cairo.

Tayanç, M., Im, U., Do ruel, M., Karaca, M., 2009. Climate change in Turkey for the last half century. Clim. Change 94 (3–4), 483–502.

Thorncroft, C.D., Flocas, H.A., 1997. A case study of Saharan cyclogenesis. Mon. Weather Rev. 125, 1147–1165.

Toreti, A., 2010. Extreme Events in the Mediterranean: Analysis and Dynamics. Ph.D. Thesis. University of Bern, Switzerland.

Toreti, A., Desiato, F., 2008. Changes in temperature extremes over Italy in the last 44 years. Int. J. Climatol. 28 (6), 733–745.

Toreti, A., Desiato, F., Fioravanti, G., Perconti, W., 2010a. Seasonal temperatures over Italy and their relationship with low-frequency atmospheric circulation patterns. Clim. Change 99 (1–2), 211–227.

Toreti, A., Xoplaki, E., Maraun, D., Kuglitsch, F.G., Wanner, H., Luterbacher, 2010b. Characterisation of extreme winter precipitation in Mediterranean coastal sites and associated anomalous atmospheric circulation patterns. Nat. Hazards Earth Syst. Sci. 10, 1037–1050.

Trenberth, K.E., Jones, P.D., Ambenje, P., Bojariu, R., Easterling, D., Klein Tank, A., et al., 2007. Observations: Surface and Atmospheric Climate Change. Climate Change 2007: The Physical Science Basis. In: Solomon, S., Qin, D., Manning, M., Chen, Z., Marquis, M., Averyt, K.B. (Eds.), Contribution of WG1 to the Fourth Assessment Report of IPCC. Cambridge University Press, Cambridge, UK, New York, NY.

Trewartha, G.T., Horn, L.H., 1980. An Introduction to Climate, fifth ed. McGraw-Hill, New York, NY, pp. 148–156.

Trigo, I.F., 2006. Climatology and interannual variability of storm-tracks in the Euro-Atlantic sector: a comparison between ERA-40 and NCEP/NCAR reanalysis. Clim. Dyn. 26 (2–3), 127–143.

Trigo, I.F., Davies, T.D., 2002. Meteorological conditions associated with sea surges in Venice. Int. J. Climatol. 22, 787–803.

Trigo, I.F., Davies, T.D., Bigg, G.R., 1999. Objective climatology of cyclones in the Mediterranean region. J. Clim. 12 (6), 1685–1696.

Trigo, I.F., Bigg, G.R., Davis, T.D., 2002a. Climatology of cyclogenesis mechanisms in the Mediterranean. Mon. Weather Rev. 130, 549–569.

Trigo, R.M., Osborn, T.J., Corte-Real, J.M., 2002b. The North Atlantic Oscillation influence on Europe: climate impacts and associated physical mechanisms. Clim. Res. 20, 9–17.

Trigo, R.M., Pozo-Vásquez, D., Osborn, T.J., Castro-Díez, Y., Gámiz-Fortis, S., Esteban-Parra, M.J., 2004. North Atlantic Oscillation influence on precipitation, river flow and water resources in the Iberian Peninsula. Int. J. Climatol. 24, 925–944.

Trigo, R.M., Xoplaki, E., Zorita, E., Luterbacher, J., Krichak, S.O., Alpert, P., et al., 2006. Relations between variability in the Mediterranean region and mid-latitude variability. In: Lionello, P., Malanotte-Rizzoli, P., Boscolo, R. (Eds.), The Mediterranean Climate: An Overview of the Main Characteristics and Issues. Elsevier, Amsterdam, pp. 179–226.

Tsidulko, M., Alpert, P., 2001. Synergism of upper-level potential vorticity and mountains in Genoa lee cyclogenesis—a numerical study. Meteorol. Atmos. Phys. 78, 261–285.

Tsvieli, Y., Zangvil, A., 2005. Synoptic climatological analysis of "wet" and "dry" Red Sea troughs over Israel. Int. J. Climatol. 25, 1997–2015.

Türkes, M., Erlat, E., 2003. Precipitation changes and variability in Turkey linked to the North Atlantic Oscillation during the period 1930–2000. Int. J. Climatol. 23, 1771–1796.

Türkes, M., Erlat, E., 2009. Winter mean temperature variability in Turkey associated with the North Atlantic Oscillation. Meteorol. Atmos. Phys. 105 (3–4), 211–225.

Uccellini, L.W., Kocin, P.J., 1987. The interaction of jet streak circulations during heavy snow events along the east coast of the United States. Weather Forecasting 2, 289–308.

Ulbrich, U., Christoph, M., Pinto, J.G., Corte-Real, J., 1999. Dependence of winter precipitation over Portugal on NAO and baroclinic wave activity. Int. J. Climatol. 19, 379–390.

Ulbrich, U., Leckebusch, G.C., Pinto, J.G., 2009. Extra-tropical cyclones in the present and future climate: a review. Theor. Appl. Climatol. 96, 117–131.

Ullmann, A., Moron, V., 2007. Weather regimes and sea level variations over Gulf of Lions (French Mediterranean coast) during the 20th century. Int. J. Climatol. 28 (2), 159–171. doi: 10.1002/joc.1527.

Vautard, R., Yiou, P., D'Andrea, F., de Noblet, N., Viovy, N., Cassou, C., et al., 2007. Summertime European heat and drought waves induced by wintertime Mediterranean rainfall deficit. Geophys. Res. Lett. 34 (7), L07711.

Wallace, J., Gutzler, D., 1981. Teleconnections in the geopotential height field during the Northern hemisphere winter. Mon. Weather Rev. 109, 784–812.

Washington, R., Todd, M.C., 2005. Atmospheric controls on mineral dust emission from the Bodélé Depression, Chad: the role of the low level jet. Geophys. Res. Lett. 32, L17701.

Webster, P.J., 1994. The role of hydrological processes in ocean–atmosphere interactions. Rev. Geophys. 32 (4), 427–476.

Winstanley, D., 1972. Sharav. Weather 27, 146–160.

Woollings, T., Hannachi, A., Hoskins, B., 2010. Variability of the North Atlantic eddy-driven jet stream. Q. J. R. Meteorol. Soc. 136 (649), 856–868.

Xoplaki, E., 2002. Climate Variability over the Mediterranean. Ph.D. Thesis. University of Bern, Switzerland.

Xoplaki, E., Gonzalez-Rouco, J.F., Luterbacher, J., Wanner, H., 2003. Mediterranean summer air temperature variability and its connection to the large-scale atmospheric circulation and SSTs. Clim. Dyn. 20 (7), 723–739.

Yaalon, D.H., Ganor, E., 1979. East Mediterranean trajectories of dust-carrying storms from the Sahara and Sinai. In: Morales, C. (Ed.), Saharan Dust. Wiley, Chichester, pp. 187–193.

Yiou, P., Nogaj, M., 2004. Extreme climatic events and weather regimes over the North Atlantic: when and where? Geophys. Res. Lett. 31 (7), L07202.

Yiou, P., Vautard, R., Naveau, P., Cassou, C., 2007. Inconsistency between atmospheric dynamics and temperatures during the exceptional 2006/2007 fall/winter and recent warming in Europe. Geophys. Res. Lett. 34 (21), L21808.

Zampieri, M., D'Andrea, F., Vautard, R., Ciais, P., de Noblet-Ducoudré, N., Yiou, P., 2009. Hot European summers and the role of soil moisture in the propagation of Mediterranean drought. J. Clim. 22 (18), 4747–4758.

Zangvil, A., Druian, P., 1990. Upper air trough axis orientation and the spatial distribution of rainfall over Israel. Int. J. Climatol. 10, 57–62.

Zecchetto, S., De Biasio, F., 2007. Sea surface winds over the Mediterranean basin from satellite data (2000–04): Meso- and local-scale features on annual and seasonal time scales. J. Appl. Meteorol. Climatol. 46, 814–827.

Ziv, B., 2001. A subtropical rainstorm associated with a tropical plume over Africa and the Middle-East. Theor. Appl. Climatol. 69, 91–102.

Ziv, B., Saaroni, H., 2011. The contribution of moisture to heat stress in a period of global warming: the case of the Mediterranean. Clim. Change doi: 10.1007/s10584-009-9710-3.

Ziv, B., Saaroni, H., Alpert, P., 2004. The factors governing the summer regime of the eastern Mediterranean. Int. J. Climatol. 24, 1859–1871.

Ziv, B., Dayan, U., Sharon, D., 2005a. A mid-winter, tropical extreme flood-producing storm in southern Israel: synoptic scale analysis. Meteorol. Atmos. Phys. 88, 53–63. doi: 10.1007/s00703-003-0054-7.

Ziv, B., Saaroni, H., Baharad, A., Yekutieli, D., Alpert, P., 2005b. Indications for aggravation in summer heat conditions over the Mediterranean Basin. Geophys. Res. Lett. 32, L12706.

Ziv, B., Saaroni, H., Yair, Y., Ganot, M., Baharad, A., Isaschari, D., 2009. Atmospheric factors governing winter thunderstorms in the coastal region of the Eastern Mediterranean. Theor. Appl. Climatol. 95, 301–310.

Ziv, B., Saaroni, H., Romem, M., Heifetz, E., Harnik, N., Baharad, A., 2010. Analysis of conveyor belts in winter Mediterranean cyclones. Theor. Appl. Climatol. 99 (3–4), 441–455.